REPORT DOCUMENTATION PAGE

1a. REPORT SECURITY CLASSIFICATION: Unclassified	1b. RESTRICTIVE MARKINGS
	3. DISTRIBUTION/AVAILABILITY OF REPORT: Approved for public release; distribution unlimited.
	5. MONITORING ORGANIZATION REPORT NUMBER(S): ARO 24480.25-EL
6a. NAME OF PERFORMING ORGANIZATION: UNIVERSITY OF CALIFORNIA; 6b. OFFICE SYMBOL (If applicable):	7a. NAME OF MONITORING ORGANIZATION: U. S. Army Research Office
6c. ADDRESS (City, State, and ZIP Code): DEPT. OF ELECTRICAL & COMPUTER ENGINEERING, UNIVERSITY OF CALIFORNIA, SANTA BARBARA, CA 93106	7b. ADDRESS (City, State, and ZIP Code): P. O. Box 12211, Research Triangle Park, NC 27709-2211
8a. NAME OF FUNDING/SPONSORING ORGANIZATION: U. S. Army Research Office; 8b. OFFICE SYMBOL (If applicable):	9. PROCUREMENT INSTRUMENT IDENTIFICATION NUMBER: DAAL03-87-K-0012
8c. ADDRESS (City, State, and ZIP Code): P. O. Box 12211, Research Triangle Park, NC 27709-2211	10. SOURCE OF FUNDING NUMBERS: PROGRAM ELEMENT NO. / PROJECT NO. / TASK NO. / WORK UNIT ACCESSION NO.

11. TITLE (Include Security Classification): High Speed Quantum-Well Optoelectronic Devices by MBE

12 PERSONAL AUTHOR(S): Larry A. Coldren

13a. TYPE OF REPORT	13b. TIME COVERED	14. DATE OF REPORT (Year, Month, Day)	15. PAGE COUNT
Final	FROM 10/23/86 TO 7/31/89	May 89	50

16. SUPPLEMENTARY NOTATION: The view, opinions and/or findings contained in this report are those of the author(s) and should not be construed as an official Department of the Army position, policy, or decision, unless so designated by other documentation.

17. COSATI CODES		
FIELD	GROUP	SUB-GROUP

18. SUBJECT TERMS (Continue on reverse if necessary and identify by block number)

19 ABSTRACT (Continue on reverse if necessary and identify by block number)

The work has involved the use of Molecular Beam Epitaxy to grow precisely controlled thin layers of III-V compound semiconductors for applications in high-speed optoelectronic devices. The program was intended to serve as a hardware complement to optical computing and high-speed signal processing systems work funded elsewhere under SDIO.

The focus of the work has been on the growth, processing and characterization of novel quantum-confined structures. In the past, such quantum-well or quantum-wire structures had been shown to hold great promise for advanced device applications, but until recently very little of this promise had been fulfilled. Partly as a result of this program, some of the desirable characteristics of such structures have been realized for the first time. For example, the first clear measurements of lateral quantum-confinement in quantum-wire arrays were obtained on layers grown by sub-atomic layer epitaxy on off-axis substrates. The body of work has been concerned with creating and evaluating novel *waveguided* as well as *surface-emitting* (transverse) device structures. In both areas, significant advances have resulted as well. Surface-emitting lasers with segmented periodic-gain have led to record low threshold pumping levels.

The report begins with a summary of the quality and characteristics of the AlGaAs and InGaAs quantum-well material that is being grown in the new ARO-GenII MBE. It then proceeds with a review of some experimental and theoretical results for quantum-wire and strained-layer structures, including lasers. In the third section novel transverse modulators and lasers that use vertical Fabry-Perot cavities are discussed, and in the final section the work with novel guided wave structures is summarized.

20 DISTRIBUTION/AVAILABILITY OF ABSTRACT: ☑ UNCLASSIFIED/UNLIMITED ☐ SAME AS RPT. ☐ DTIC USERS	21. ABSTRACT SECURITY CLASSIFICATION: Unclassified
22a. NAME OF RESPONSIBLE INDIVIDUAL: Larry A. Coldren	22b. TELEPHONE (Include Area Code): (805) 961-4486; 22c. OFFICE SYMBOL

ARO 24480.25-EL-SDI

High Speed Quantum-Well optoelectronic Devices by MBE

ARO-DAAL03-87-K-0012 - FINAL REPORT

3/1/88-5/31/89

by

L.A. Coldren: Principal Investigator
H. Kroemer & J.L. Merz: Associate Investigators
J.H. English & D. Cohen : Development Engineers
R.S. Geels, R. J. Simes, S. Corzine, T.C. Huang,
T. Hausken & W. Zou: Students
J.M. Gaines & M. Tsuchiya: Visiting Research Engineers

ECE Technical Report #89-07

Department of Electrical & Computer Engineering

University of California at Santa Barbara

May 1989

Table of Contents

A. Introduction & Problem Statement

This is the final report on DAAL03-87-K-0012 which ended March 31, 1989. The work has involved the use of Molecular Beam Epitaxy to grow precisely controlled thin layers of III-V compound semiconductors for applications in high-speed optoelectronic devices. The program was intended to serve as a hardware complement to optical computing and high-speed signal processing systems work funded elsewhere under SDIO.

The focus of the work has been on the growth, processing and characterization of novel quantum-confined structures. In the past, such quantum-well or quantum-wire structures had been shown to hold great promise for advanced device applications, but until recently very little of this promise had been fulfilled. Partly as a result of this program, some of the desirable characteristics of such structures have been realized for the first time. For example, the first clear measurements of lateral quantum-confinement in quantum-wire arrays were obtained on layers grown by sub-atomic layer epitaxy on off-axis substrates. In fact, the world's first quantum-wire lasers were recently demonstrated with such material. These are clearly breakthrough results. However, these are but two examples of progress that will be summarized in this report. The body of work has been concerned with creating and evaluating novel *waveguided* as well as *surface-emitting* (transverse) device structures. In both areas, significant advances have resulted as well. As a final example, consider the proposal of surface-emitting lasers with segmented periodic-gain. This structure has led to record low threshold pumping levels. It currently is being widely imitated.

The report begins with a summary of the quality and characteristics of the AlGaAs and InGaAs quantum-well material that is being grown in our new ARO-GenII MBE. It then proceeds with a review of some experimental and theoretical results for quantum-wire and strained-layer structures, including lasers. In the third section novel transverse modulators and lasers that use vertical Fabry-Perot cavities are discussed, and in the final section the work with novel guided wave structures is summarized.

B. Summary of Accomplishments

I. MBE Materials growth & characterization

a. General growth characteristics

For the successful growth of novel optoelectronic device structures, we have worked to make sure that we can grow good material and quantum well lasers that have good photoluminescence characteristics. In Fig. I.1, we show photoluminescence data for a multiquantum-well sample; the peak at 6468 Å can be ascribed to emission from a quantum well approximately 10 Åwide. Its full-width-at-half-maximum is 14 meV, which is state-of-the-art [I.1] for such a narrow well, indicative of the smoothness of the layers at the heterointerface. Our laser effort has been concentrated on quantum well lasers. Fig I.2 is a light-current plot and a current-voltage curve for a broad-area graded-index-separate-confinement-heterostructure (GRINSCH) laser. Its threshold current density is 270 A/cm^2, a value comparable to the lowest ever achieved for a structure with the thicknesses and compositions used. (Lower values have been obtained by using much higher Al content in the cladding regions in very long devices.)

Another measure of epilayer quality is the mobility which can be achieved in a modulation doped structure. To this end we have pursued the growth and characterization of such high mobility structures and have obtained 4 K mobilities as high as 1 x 10^6 cm^2/V-s using a 450 Å undoped setback as illustrated in Fig. I.3. This high mobility is an indicator of extreme material purity and is comparable to the highest values ever achieved.

b. Automation package

In order to facilitate the reliable growth of complicated heterostructures, such as those mentioned above, an extensive software program (called MBE Master) was developed. Shutters, oven temperature set points, substrate temperature, substrate position, and substrate rotation speed are all under software control. MBE Master includes a full screen editor which permits the user to specify a series of commands (called a growth program) by typing text.

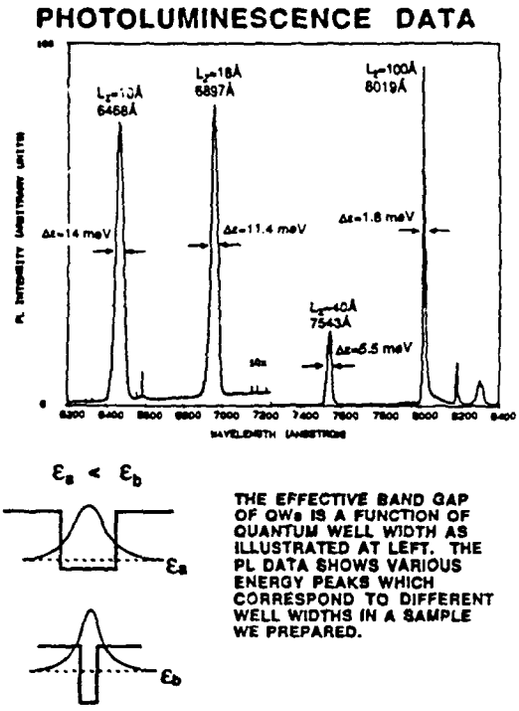

Fig. I. 1. Photoluminescence data for a multiquantum-well sample.

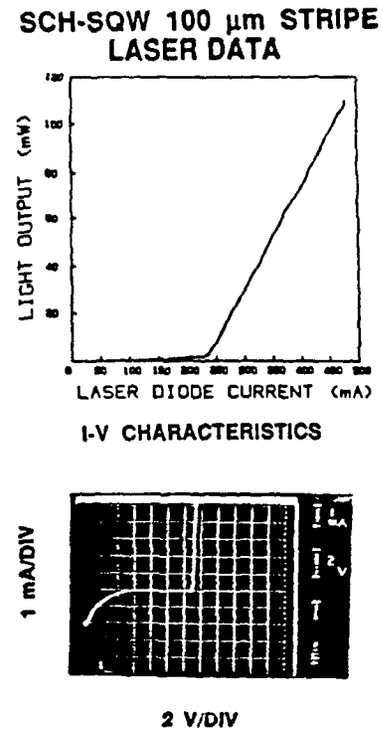

Fig. I. 2. A light-current plot and a current-voltage curve for a broad-area graded-index-separate-confinement-heterostructure (GRINSCH) laser.

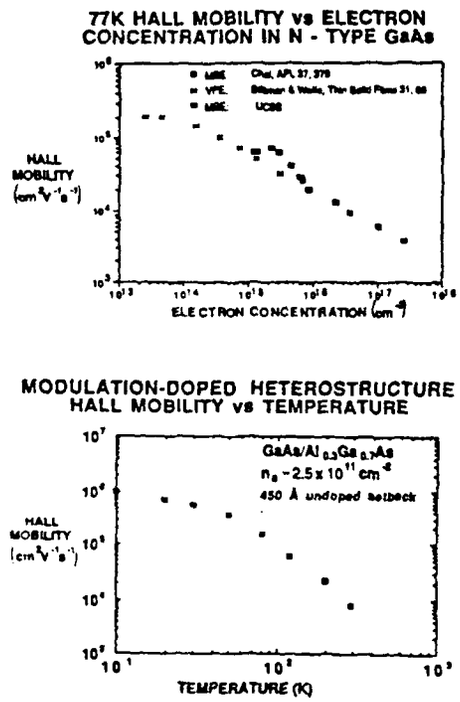

Fig. I. 3. The growth and characterization of high mobility structures

The growth rate of every material to be grown is specified at the beginning of the growth program and then each layer is specified on a subsequent line by defining which material is to be grown, the thickness of the layer, and the dopant source if any. In addition to specifying the layers, commands such as rotation speed, time delays, and oven setpoint changes can be included at any point in the growth.

After the growth program is complete it can be stored on a hard disk for immediate recall at a later time or it can be executed. When the growth commences, MBE Master compiles the growth program and puts up a graphic display indicating which shutters are open, current oven temperatures and other details. The growth then proceeds totally without operator assistance and the user is notified when it is complete.

The MBE Master program has made it possible to repeatably and reliably grow structures with arbitrary levels of complication. The user can specify nested loops and even subprograms so that growth programs for complex structures are compact and easy to enter.

c. Parabolic quantum-well structure

Another interesting structure that has been studied in the ARO MBE is the grown-in parabolic well. In work partially funded by AFOSR this has been done by using the computer to "digitally" chop the material x-value in order to obtain a parabolic grading of the potential. Then when the material outside the well is doped the well fills up with electrons and the bottom flattens out resulting in a uniform three-dimensional electron gas. This then allows studies of the physics of a high mobility 3-D electron gas.

d. Low temperature laser growth

The conventional wisdom for growth of lasers by MBE is that a high substrate temperature (~700°C) is required for low-threshold current density lasers. However, high growth temperatures are undesirable for several reasons: increased dopant diffusion, gallium reevaporation (which can make control of x-values more difficult), and increased incompatibility with the growth of lasers with InGaAs active layers. For example, in one

structure that we have been studying, the surface-emitting laser with periodic gain, the total epi-layer thickness can be quite high and there may be several highly-doped p-type layers. Dopant diffusion during growth can be a difficult problem to control. Thus, we have worked on growing lasers by MBE at relatively low growth temperatures. We have pursued two avenues: use of superlattice layers for the laser cladding layers and use of a new high-purity aluminum source for growth of our AlGaAs. Regarding the use of superlattice (SL) cladding layers, we have achieved good results in conventional GaAs-active double heterostructure lasers with threshold current densities of ~800A/cm^2 in lasers growth at temperature of 540°C (again near state-of-the-art for this configuration)[I.2].

In control samples using growth at low temperatures with conventional alloy cladding layers, lasing was either not observed or occurred erratically at high threshold current densities. We attribute the low laser thresholds in our SL samples to trapping of impurities that could act as non-radiative recombination centers. We have also tried the SL approach for growth of lasers with quantum well active layers; however, the SL approach does not seem to improve laser quality in QW laser samples grown at low substrate temperatures. Photoluminescence studies are currently under way to attempt to understand the observed data. We have also recently installed a new high purity aluminum source in the ARO Gen II [I.3]. Y. Shiraki and coworkers demonstrated that they could grow AlGaAs at low temperatures and see good photoluminescence properties. We have grown a single quantum well separate confinement heterostructure laser at a substrate temperature of 600°C; it has a threshold current density of ~550 A/cm^2, a relatively low value which indicates the promise of the high purity aluminum source for laser growth. Lasers grown at such a low temperature with our old aluminum source did not lase. We have not tried to grow a laser structure at lower temperatures, although one might expect substrate temperatures in the 500°C range to be possible.

e. GaInAs strained-layer QW lasers

Recently there has been increasing interest in the potential of pseudomorphic strained-

layer materials for use in electronic and optoelectronic applications. It has been shown theoretically [I.4] that replacing a normal unstrained quantum well with a strained material in a laser can decrease the threshold current density of the device. We have also recently shown that the relaxation frequency can also be quite high in such structures [I.5]. Experimentally, we have made progress toward incorporating GaInAs quantum wells in lasers. Broad area lasers have been fabricated from a laser structure incorporating a single 80 Å$Ga_{0.8}In_{0.2}As$ quantum well. Results are shown in Fig. I.4. The threshold current density for this SCH was 530 A/cm^2 and the single facet differential quantum efficiency was 30%. The lasing wavelength was 0.995 μm. Current efforts with strained layers include incorporation into vertical cavity surface emitting lasers and plans for use in Fabry-Perot modulators and other optoelectronic devices.

f. Tilted Superlattices by MBE

Low dimensional structures having quantum confinement in two or three dimensions such as quantum well wires (QWW's) and quantum well boxes have in the last few years attracted much attention not only for their potential in uncovering new phenomena in solid state physics but also for their potential device applications. A new approach to control the nucleation and growth kinetics available with molecular beam epitaxy (MBE) on vicinal substrates has made possible the direct growth of lateral superlattices. The lateral dimensions in those structures are in the low nanometer range and match the requirement for device applications. It is currently the only technique to make QWW arrays with these dimensions, and initial measurements, as reported in the following, suggest that it may be an extremely powerful technique for QWW device structures.

We have demonstrated successfully for the first time GaAs/AlAs superlattices having interface planes tilted with respect to the substrate surface plane [I.6]. The amount of tilt and the superlattice period can be controlled by adjusting the growth parameters (see Fig.I.5). TSL's were produced by depositing fractional monolayer superlattices $(GaAs)_m(AlAs)_n$, with

p=m+n − 1, on vicinal (001) substrates. The TSL was clearly observed in the transmission electron microscopy cross section of the sample.

We also observed spontaneous growth of coherent tilted superlattice on vicinal (001) GaAs substrates [I.7]. Periodic Al composition modulations have been formed spontaneously during MBE of AlGaAs on vicinal (001) substrates. The formation of the Al modulation requires one monolayer - coherent deposition of Al and Ga atoms per cycle by migration enhanced epitaxy (C-MEE, see Fig. I.6 (a)). Hence the denomination of coherent tilted superlattice (C-TSL). In Fig. I.6 (b), cross sectional transmission electron microscopy clearly shows that the C-TSL has the periodicity of the surface steps. We clarified that the Al rich regions of the C-TSL form at the bottom of steps before the As flux is established. This is one of clear evidences that growth kinetics and bonding nature of Al and Ga atoms on the steps play important roles in MBE.

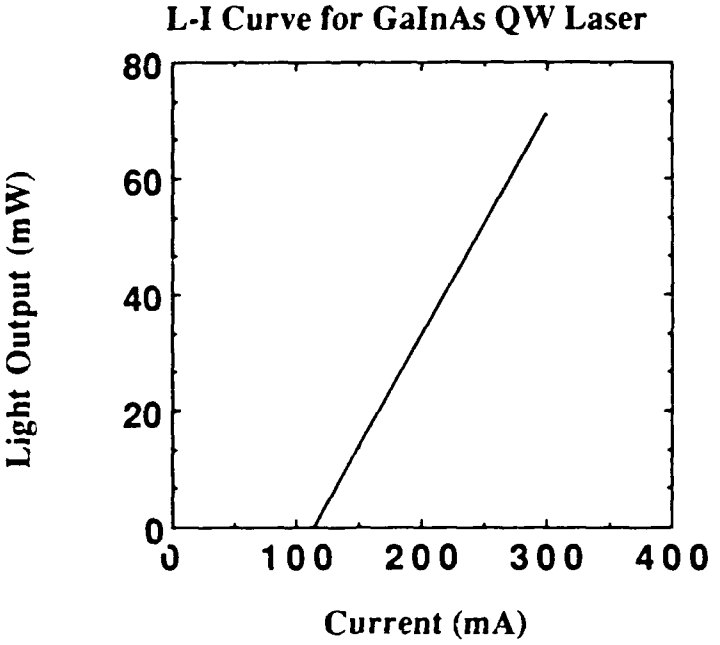

Fig. I. 4. Broad area strained-layer QW laser L-I characteristic. In percentage = 20%. Device is 50 μm long by 380 μm wide

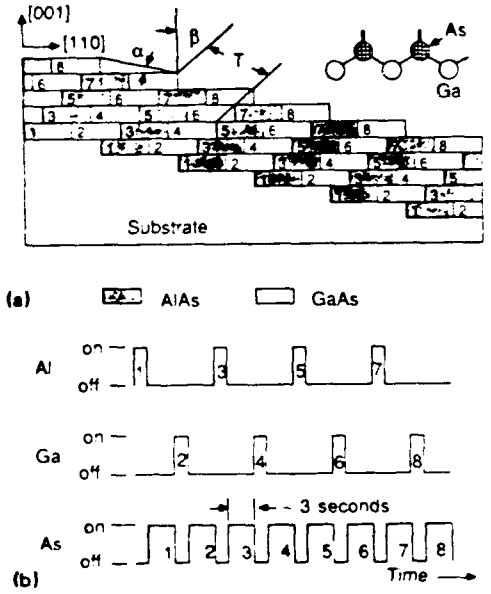

Fig. I. 5. Idealized representation of a tilted superlattice grown by alternating-beam deposition. (a) Cross section, perpendicular to the step edges, of a superlattice with p = 1.25. The inset shows the arrangement of the As bonds with respect to the step edges. (b) Detail of growth, showing the order of atomic depositions. Numbers in (a) refer to partial monolayers deposited in (b).

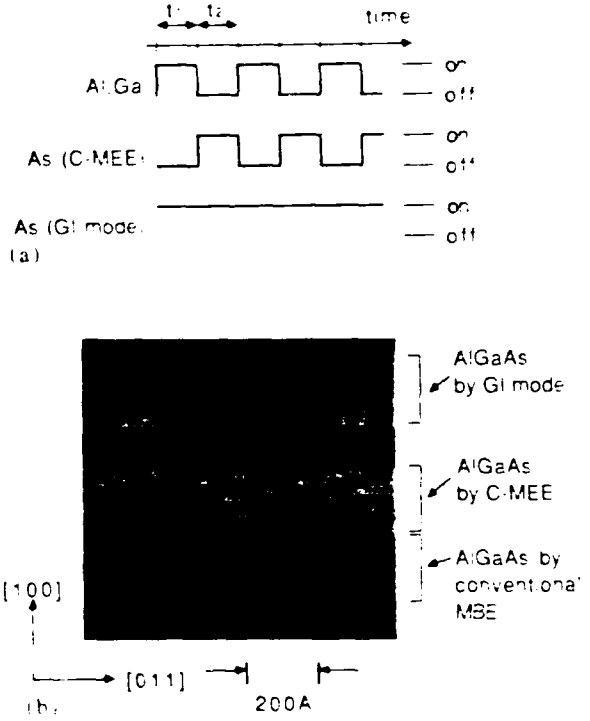

Fig. I. 6. (a) Schematic of the shutter opening and closing sequences for the C-MEE mode and for the GI mode where growth interruption is introduced after each one monolayer MBE deposition of Al and Ga with As flux. (b) Dark field TEM cross-section micrograph of AlGaAs layers grown on a 1° off wafer by MBE, in the C-MEE mode, and the GI mode. The operating Bragg reflection is ⟨200⟩. The Al-rich regions correspond to the lighter areas in the micrograph.

References for section I:

[I.1] G. Weimann, *Physica* **129B**, 459 (1985).

[I.2] "GaAs/AlxGa1-xAs Lasers Grown by Molecular Beam Epitaxy at Low Substrate Temperatures," R. J. Simes, P. O. Holtz, F. Laruelle, L. A. Coldren, J. H. English, and A. C. Gossard, *1989 Electronic Materials Conference*, Boston, MA (June 1989).

[I.3] Y. Shiraki, T. Mishima. and M. Morioka, *J. Crystal Growth* **81**, 164 (1987)

[I.4] "Reduction of lasing threshold current density by the lowering of valence band effective mass," E. Yablonovitch and E. O. Kane, *J. Lightwave Technol.*, **LT-4**, p. 504 (1986).

[I.5] "Extremely wide modulation bandwidth in a low threshold current strained quantum well laser," I. Suemune, L. A. Coldren, M. Yamanishi, and Y. Kan, *Appl. Phys. Lett.*, **53**, 1380 (1988).

[I.6] "Molecular-beam epitaxy growth of tilted GaAs/AlAs superlattices by deposition of fractional monolayers on vicinal (001) substrates", J. M. Gaines, P. M. Petroff, H. Kroemer, R. J. Simes, R. S. Geels, and J. H. English, *J. Vac. Sci. Technol.* **B6**, 1378(1988).

[I.7] "Spontaneous growth of coherent tilted superlattice on vicinal (100) GaAs substrates", M. Tsuchiya, P. M. Petroff, and L. A. Coldren, *Appl. Phys. Lett.* **54**, 1690(1989).

II. Quantum-Well-Wire and Strained-layer Calculations and Measurements

a. Optical properties of quantum well wires using TSL's and QWW lasers

The performance of optical devices with quantum-well-wires and quantum-well-boxes is expected to exceed those with quantum well layer structures in many aspects. However, to realize the predicted superior properties, in-plane dimensions in the low nanometer range, in addition to small vertical sizes, are required. The lateral dimensions of TSL's as introduced above are typically in the low-nanometer range (~ 20 - 100 Å) and suitable for QWW device applications.

We designed a QWW array shown in the inset of Fig. II.1 on a vicinal (001) semi-insulating GaAs substrate tilted 2° toward [110]; the average step size is 8 nm. In this structure, carriers are expected to be pushed from the TSL region to the GaAs layer and be confined laterally by the potential variation of the TSL (~ 4 nm GaAs / 4 nm AlAs). Quantum level broadening due to the step size fluctuation is calculated to be smaller because of the relatively weak lateral confinement as compared to QWW's with fully surrounding AlAs barriers. A photoluminescence (PL) study was carried out on this structure. A strong anisotropy was observed in the ratio of the electron-light hole exciton peak intensity to the electron - heavy hole exciton peak intensity in PL excitation spectra whereas no polarization dependence was observed in a single quantum well as shown in Fig.II.2 [II.1]. Relative matrix elements of optical transitions were calculated by taking the optical selection rules into account. The observed optical anisotropy was well explained by the theory. These results constitute the first evidence of two dimensional *quantum* confinement in artificial wire structures having cross-sectional dimensions in the nanometer range. The data show that such QWW structures have great promise for use in novel optical devices.

Lasers with quantum-well-wire (QWW) active regions have been demonstrated using the tilted superlattice (TSL) structures [II.2, II.3]. The TSL-QWW's consist of a 5 nm GaAs layer and a 5 nm AlGaAs (x = 0.25) - GaAs TSL layer which are sandwiched by AlGaAs (x = 0.25)

waveguide and AlGaAs (x = 0.5) cladding layers (see Fig. II.1). Experimental results are shown in Fig. II.3. Threshold current density as low as 470 A/cm^2 and differential quantum efficiency of 22 % per facet were obtained in a laser thus fabricated with a long cavity (990 μm) at room temperature. The lasing wavelength was 827.7 nm which corresponds to the QWW state energy. Measured modal gain spectra were as narrow as those of typical single QW lasers. Characteristic temperatures T_0 were 80 - 130 °K. Although superior properties of QWW lasers were not observed, due to both nonoptimal device geometry and MBE growth parameters, the quality of the TSL-QWW is still high enough to demonstrate good lasers. This is the first report of lasing action in a laterally structured device in which unambiguous lateral confinement of carriers exists. We have also observed clear exciton absorption in the TSL-QWW's at room temperature, which leads to possible optical devices using excitonic effects.

b. Extremely wide modulation bandwidth in a low threshold current strained quantum well laser

Lasing characteristics of strained quantum well (QW) structures such as InGaAs/AlGaAs on GaAs and InGaAs/InAlAs on InP were analyzed by taking into account the band mixing effect in the valence band. A relaxation oscillation frequency f_r, which gives a measure of the upper modulation frequency limit, was found to be increased by 3 times in a 50Å $In_{0.9}Ga_{0.1}As/In_{0.52}Al_{0.48}As$ QW structure compared with that in a 50Å $GaAs/Al_{0.4}Ga_{0.6}As$ QW structure for the undoped case. One of the main factors for this improved frequency band width is attributed to the reduced subband nonparabolicity as well as the reduced valence band density of states in the strained QW structure. The corresponding lasing threshold current is one-order of magnitude smaller than that of the GaAs/AlGaAs QW structure. With a p-doping in the QW the f_r value increases, and the 3-dB cutoff frequency of about 90 GHz will be expected with an acceptor concentration of $5x10^{18}$ cm^{-3} in the $In_{0.9}Ga_{0.1}As/In_{0.52}Al_{0.48}As$ QW.

There has been increasing interest in the high-frequency modulation capability of

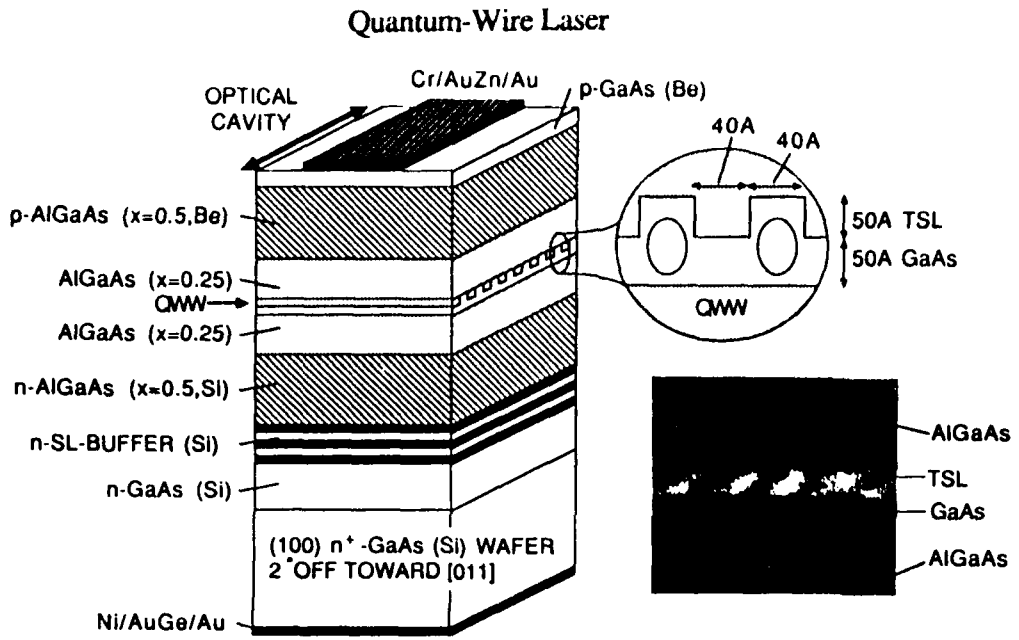

Fig. II. 1. The TSL-QWW's consist of a 5 nm GaAs layer and a 5 nm AlGaAs (x = 0.25) - GaAs TSL layer which are sandwiched by AlGaAs (x = 0.25) waveguide and AlGaAs (x = 0.5) cladding layers.

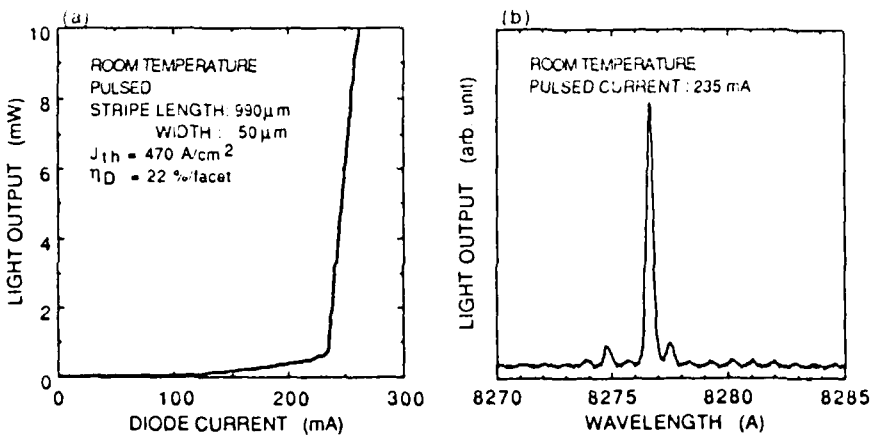

Fig. II. 3. L-I curve of a laser with a 990μm cavity at room temperature (a). lasing spectra of the laser just above the threshold (b). The spectra were measured by a grating monochromator and a photo-multiplier tube.

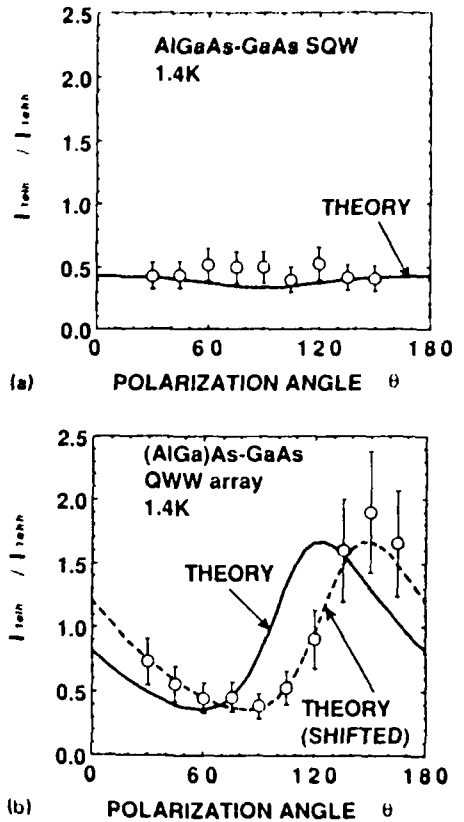

Fig. II. 2. The ratio of the area of PLE peak for electron light-hole exciton (I1elh) to that for electron heavy-hole exciton (I1ehh) is plotted as a function of θ in the SQW sample (a) and in the QWW sample (b). The solid lines show the calculated prediction. The broken line in (b) is shifted from the theoretical curve by an offset of $\Delta\theta = 25°$.

semiconductor lasers to realize high bit-rate optical fiber communication and high speed opto-electronic integration. The direct modulation bandwidth of a semiconductor laser is given by the relaxation oscillation corner frequency f_r which is of the form[II.4].

$$f_r = \frac{1}{2\pi}\sqrt{\frac{c\,G}{n_r}\frac{S_0}{\tau_p}}, \qquad (1)$$

where S_0 is the stationary photon density in the cavity, G is the differential gain (i. e., $G=\partial g/\partial n$ where g is the optical gain and n is the carrier concentration), τ_p is the photon lifetime, n_r is the refractive index of the laser medium, and c is the light velocity. There have been various attempts to increase the f_r value such as high output power operation to increase the S_0 value, quantum well (QW) structures[II.5] and low temperature operation to increase the G value, and short cavity lasers to reduce the τ_p value. In addition to these experiments to improve the laser structure and the operation conditions, p-type doping in the QW was proposed to increase the G value[II.6].

From a materials viewpoint, progress in epitaxial growth techniques has made it possible to employ a strained QW structure as an active layer of a semiconductor laser. Continuous wave room temperature operation was reported in a strained $In_{0.37}Ga_{0.63}As/Al_yGa_{1-y}As$ QW laser with the low lasing threshold current density (J_{th}) of $\sim 150 A/cm^2$ where the $In_{0.37}Ga_{0.63}As$ well layer is under a 2.6% biaxial compression[II.7]. The reduction of J_{th} was proposed theoretically in strained QW structures[II.8,9]. This was based on the reduction of the valence band effective mass by the biaxial compression in the plane of the QW, which may reduce the J_{th} value. But the theory was corrected later[II.10] so that the effective mass at the zone center is independent of the strain.

In our work we have shown for the first time the extreme high-speed capability of strained QW structures in addition to the low threshold current property from the theoretical comparisons between the strained and unstrained QW laser structures. It was found that a reduction of the valence-band effective mass comes from a lifting of the band degeneracy in the

QW structure, and that the main factor which gives the above different laser properties is the nonparabolicity in the valence-band subband structures due to the band mixing and the related increase of the valence-band density of states (DOS).

The laser properties were calculated for several material combinations of interest, i.e., two unstrained QW's of $GaAs/Al_{0.4}Ga_{0.6}As$ on GaAs and $In_{0.53}Ga_{0.47}As/InP$ on InP, and two biaxially compressed QW's of $In_{0.37}Ga_{0.63}As/Al_{0.4}Ga_{0.6}As$ on GaAs and $In_{0.9}Ga_{0.1}As/In_{0.52}Al_{0.48}As$ on InP. For the purpose of comparing the material properties, the QW width was assumed to be 50Å in all cases. The critical thickness for causing misfit dislocations in the strained $In_xGa_{1-x}As$ QW structure is estimated to be about 95Å for 2.6% biaxial compression. A threshold optical gain of 1000 cm^{-1} was assumed for all the systems to be discussed in the following. The photon lifetime is taken to be 2 ps . The TE-polarization was assumed for the gain calculation.

The calculated relaxation oscillation frequency f_r versus the p-type doping level is shown in Fig. II.4 for the four material systems. An optical output power P_{out} of 20 mW from a 2 μm wide stripe, i.e., 20 mW/(2μmx0.01μm/0.05) was assumed in the calculation, which is a feasible power level even in the strained QW laser structure[II.4]. The oscillation wavelength assumed for each system is 0.81 μm for $GaAs/Al_{0.4}Ga_{0.6}As$, 1.04 μm for $In_{0.37}Ga_{0.63}As/Al_{0.4}Ga_{0.6}As$, 1.39 μm for $In_{0.53}Ga_{0.47}As/InP$, and 1.89 μm for $In_{0.9}Ga_{0.1}As/In_{0.52}Al_{0.48}As$ which were calculated from the lowest transition energies for the 50Å QW's. In each material system in Fig. II.4, the upper and lower curves were calculated with the [100] and [110] dispersions for the subbands in the valence band, respectively. In the strained case, the difference of the two curves are small because of the reduced subband nonparabolicity and the isotropic hole mass near the QW valence-band edge. The increase of the f_r value in the undoped strained systems such as $In_{0.37}Ga_{0.63}As/Al_{0.4}Ga_{0.6}As$ and $In_{0.9}Ga_{0.1}As/In_{0.52}Al_{0.48}As$ is clearly seen in Fig. II.4. This is because the Fermi level in the valence band of the strained QW easily shifts for a change of the carrier concentration due to

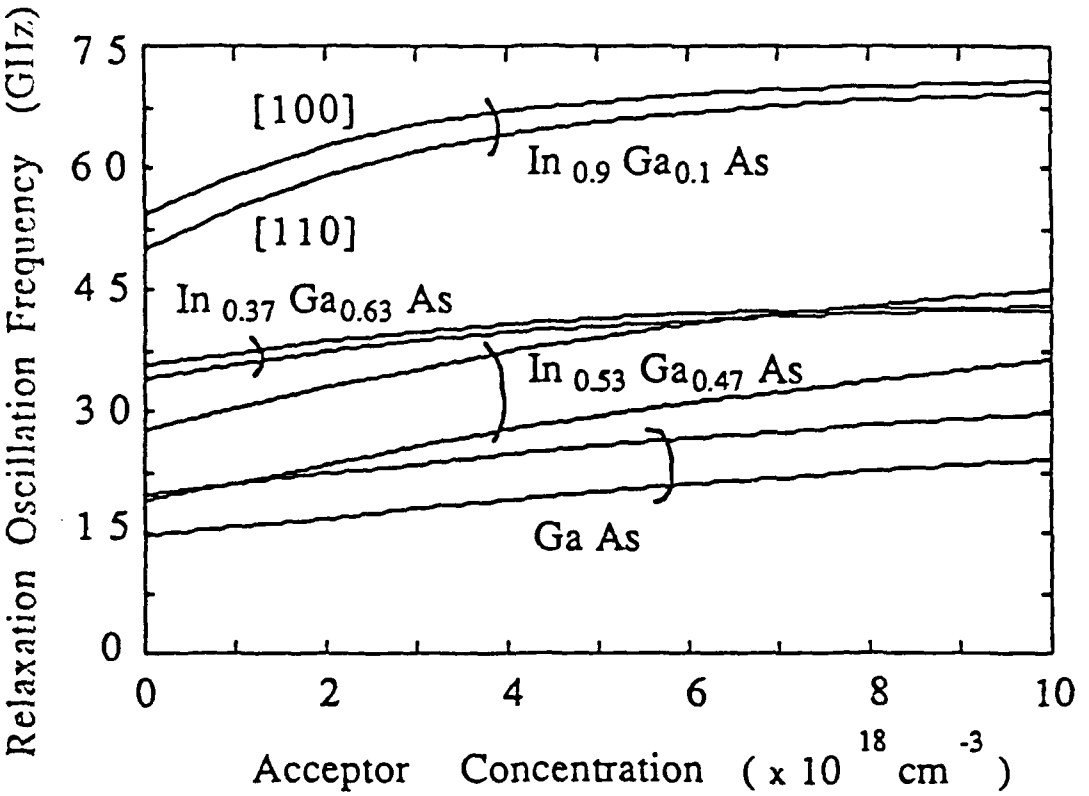

Fig. II.4 Relaxation oscillation frequency vs. acceptor concentration in the well was calculated for two unstrained QW's of GaAs/$Al_{0.4}Ga_{0.6}As$ and $In_{0.53}Ga_{0.47}As$/InP, and for two biaxially compressed QW's of $In_{0.37}Ga_{0.63}As/Al_{0.4}Ga_{0.6}As$ and $In_{0.9}Ga_{0.1}As/In_{0.52}Al_{0.48}As$. In each material system, the upper and lower curves were calculated with the [100] and [110] dispersions for the valence subbands, respectively.

the reduced DOS near the band edge as shown in Fig. II.4(b) and the resultant increase of the differential gain. The larger improvement in the $In_{0.9}Ga_{0.1}As$ system is attributed to the smaller conduction band effective mass and the longer oscillation wavelength. For the undoped $In_{0.9}Ga_{0.1}As/In_{0.52}Al_{0.48}As$ system, the f_r value is about 3 times larger than that of the $GaAs/Al_{0.4}Ga_{0.6}As$ system and it reaches as high as 67 GHz with the acceptor doping level of $5x10^{18}cm^{-3}$. Since the 3-dB cutoff frequency is given by 1.2 f_r -1.5 f_r , the 3-dB cutoff frequency near 90 GHz is expected. When the same photon density S_0 is assumed, the unstrained $GaAs/Al_{0.4}Ga_{0.6}As$ and $In_{0.53}Ga_{0.47}As/InP$ systems give almost the same f_r values. The f_r value in the GaAs system increases with p-doping of $1x10^{19}$ cm^{-3} by 70-80% compared with the undoped case, which is in reasonable agreement with the measurement[II.4].

The calculated lasing threshold current density for the $In_{0.9}Ga_{0.1}As/In_{0.52}Al_{0.48}As$ QW is about 43 A/cm^2 and is slightly reduced with the p-doping, which is about 1/9 of that for the $GaAs/Al_{0.4}Ga_{0.6}As$ QW. The assumed twin 50Å QW is not the optimum structure for the reduction of the threshold current and it will be reduced further with an adequate design. The Auger recombination which increases the threshold current in the long wavelength lasers was not included in the present calculation, but it will be effectively reduced in the strained system since the carrier concentration at threshold is $9x10^{17}$ cm^{-3} in the strained $In_{0.9}Ga_{0.1}As$ system and is reduced to ~1/3 of that in the unstrained $In_{0.53}Ga_{0.47}As$ system.

References for section II:

[II.1] "Optical anisotropy in a quantum well wire array with two dimensional quantum confinement", M. Tsuchiya, J. M. Gaines, R. H. Yan, R. J. Simes, P. O. Holtz, L. A. Coldren, and P. M. Petroff, Phys. Rev. Lett. 62, 466(1989).

[II.2] "AlGaAs/GaAs Lasers with Quantum-Wire Active Regions", M. Tsuchiya, L. A. Coldren, and P. M. Petroff, IOOC '89, Kobe, Japan (July, 1989).

[II.3] "Use of Tilted-Superlattices for Quantum-Well-Wire lasers ", M. Tsuchiya, P. M. Petroff, and L. A. Coldren, DRC '89, Boston, MA (June, 1989).

[II.4] K. Y. Lau, and A. Yariv, IEEE J. Quantum Electron. **QE-21**,121 (1985).

[II.5] Y. Arakawa, and A. Yariv, IEEE J. Quantum Electron. **QE-22**, 1887(1986).

[II.6] K. Uomi, T. Mishima, and N. Chinone, Appl. Phys. Lett. **51**, 78 (1987).

[II.7] S. E. Fischer, D. Fekete, G. B. Feak, and J. M. Ballantyne, Appl. Phys. Lett. **50**, 714 (1987).

[II.8] E. Yablonovitch and E. O. Kane, IEEE J. Lightwave Technology, **LT-4**, 504 (1986).

[II.9] A. R. Adams, Electron. Lett. **22**, 249 (1986).

[II.10] E. Yablonovitch and E. O. Kane, IEEE J. Lightwave Technology, **LT-4**, 961 (1986).

III. Novel Transverse Modulators and Lasers

a. Fabry-Perot surface-normal modulator work

Although the primary device funding for this work was provided by AFOSR, the essential materials base support was partially provided by ARO. Thus, we summarize the achievements very briefly here. As shown in Fig. III.1, the device consists of an optical cavity enclosed by quarter-wave stack dielectric mirrors which are formed in the same growth cycle in the MBE machine [III.1]. The top mirror is typically doped p-type, the bottom mirror is doped n-type and the cavity is typically filled by undoped multiple quantum-well (MQW) material. A reverse bias to this pin diode provides an electric field across the active MQW region to modulate its absorption and index of refraction. For most of the experiments the index change has been primarily used to shift the resonant frequency. This leads to a changing reflectivity for wavelengths near the Fabry-Perot resonances. To date on-off ratios >10:1 with < 10V applied and ~3dB insertion losses have been achieved.

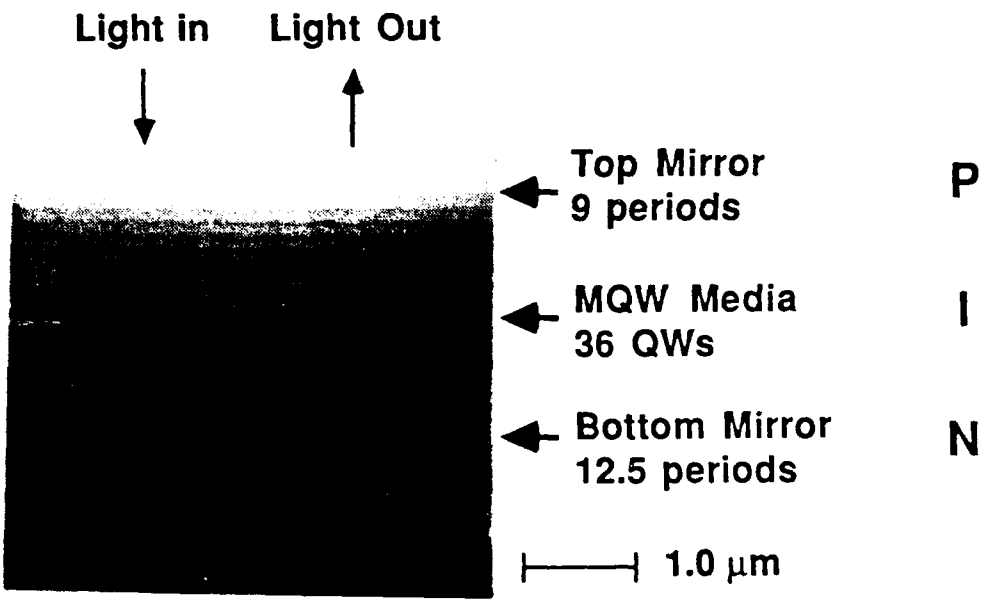

Fig. III.1. Scanning electron microscope cross-section of Fabry-Perot resonator. The two-quarter wavelength stacks (light/dark regions on photo) are separated by an MQW active layer.

b. Vertical-cavity surface-emitting-lasers

Our research in the area of vertical cavity Surface-Emitting Lasers (SEL's) can be broken down into three main components: (1) design and analysis of novel, efficient SEL structures, (2) MBE growth and optical pumping characterization of optimally designed structures, and (3) development of new fabrication processes for electrically pumping these devices. We have made considerable progress in all three areas.

Previous to our work, all SEL designs had striven to have more-or-less uniform gain along the length (vertical axis) of the active region. We introduced the concept of what is now commonly known as periodic gain [III.2]. The periodic placement of gain within the active region was analyzed and shown to provide a factor of two reduction in threshold current over ordinary uniform gain lasers [III.2, III.3]. The periodic gain concept is illustrated in Fig.III.2. With the gain material placed on half-wavelength centers along the length of the active region, it is possible to increase the net modal gain by aligning the gain segments with electric field standing wave maxima as illustrated. Since the peak of a $(\sin)^2$ function is twice its average value, we can see how a factor of two can be gained. Put another way, we save the current required to pump the material near the minima by replacing it with transparent, higher band gap layers. This configuration also has the advantage of having a much larger modal gain for one particular longitudinal mode since the periodic gain segments match only the standing wave pattern of this one mode. This factor, in fact, becomes the dominant mechanism of mode selection in our scheme. Using modern MBE or MOCVD technology it is easy to implement such a periodic gain structure.

We implemented our periodic gain design by growing SEL wafers using the ARO Varian Gen II MBE machine. The first optical pumping results performed on our samples demonstrated the lowest power density lasing threshold reported at that time [III.3-III.6]. Very narrow spectral line widths were also observed on these samples (see Fig. III.3). These initial measurements were performed at Sandia National Labs in a collaborated effort. The lowest

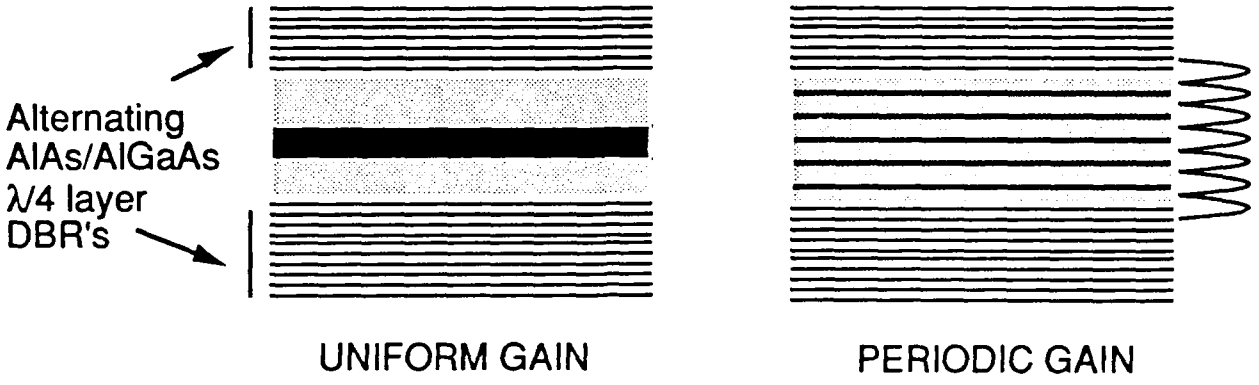

Fig.III.2 Schematic of Uniform and Periodic Gain SEL's. The active regions are indicated in black. In the PG structure, the active regions are lined up with the optical standing wave peaks, which are illustrated at the right. Light propagates back and forth in the vertical direction.

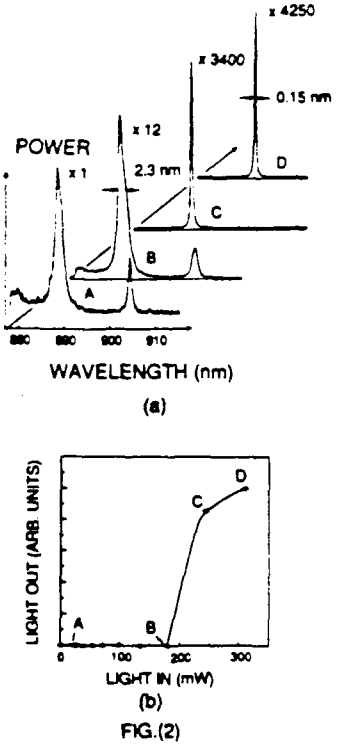

Fig.III.3 Room temperature optical pumping results on periodic gain DBR-SEL test wafers. (a) Spectra of the light emitted from the samples for steadily increasing dye laser pump powers. (b) Light-in (incident on sample) versus light-out (L-L). The spot size of the input light was 10 μm which leads to a threshold input power density of $2\text{-}3 \times 10^4$ W/cm^2 (after including input power lost to reflection, and not absorbed in the active region).

optical power density threshold measured was 2-3 x $10^4 W/cm^2$, a factor of five lower than previously reported results. The wafers consisted of grown-in distributed Bragg reflectors with $Al_{0.2}Ga_{0.8}As$/AlAs alternating quarter-wave layers. The cavity itself consisted of 20 - 600 Å GaAs active segments separated by $Al_{0.3}Ga_{0.7}As$ passive segments much like that depicted in Fig.(III.2).

We have since then set up our own optical pumping system capable of fully characterizing our MBE grown SEL wafers. We can now measure optical power density lasing thresholds in both pulsed and CW mode. We can also measure external quantum efficiency, near and far-field patterns, and emission spectra below and above threshold. The system serves as a convenient tool for quick evaluation of our just-grown wafers. Non-uniformities in MBE growth make it such that lasing action occurs more efficiently on some areas of the wafer than others. Our optical pumping system has been used to determine the best areas of the wafer which can then be cleaved up and used for actual fabrication of devices.

Recently, we have used our optical pumping system to perform the first direct experimental comparison of two optimally designed Distributed Bragg Reflector Fabry-Perot Surface-Emitting Lasers (DBR-SEL), one with a periodic gain (PG) active region and the second with a uniform gain (UG) active region of equal gain and cavity length [III.7]. The lasing characteristics of both structures demonstrated very low power density thresholds (< $10^5 W/cm^2$) as well as narrow above threshold spectral line width (< However, the threshold power density of the PG configuration was found to be approximately 30% lower than the UG configuration, the lowest threshold being 45–55kW/cm^2 under pulsed mode operation (1 μs, 100kHz) (see Fig.III.4). The differential quantum efficiency of both configurations was measured to be ~15% with peak output powers exceeding 30 mW. The above threshold far-field angle of both configurations was measured to be ~6°full angle corresponding to a 10 μm spot size, in agreement with the measured spot size. The small divergence angles make these SEL's ideal for coupling light into optical fibers with minimal loss (see Fig.III.5).

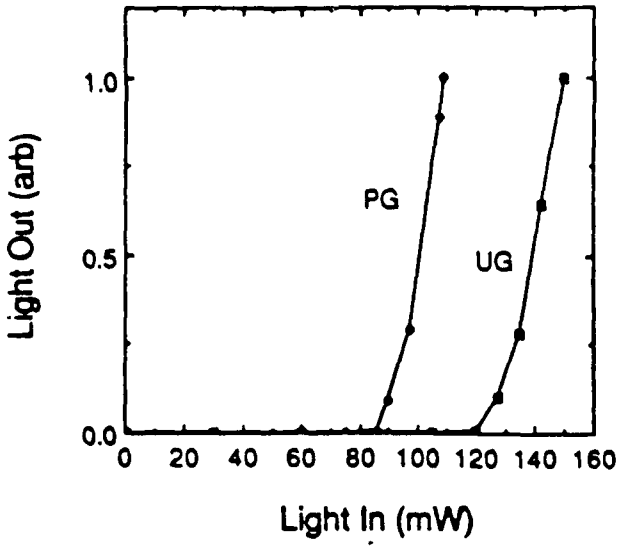

Fig.III.4 L-L curves for both the PG and the UG. The full scale vertical axis corresponds roughly to 2 mW. The PG structure consistently produced threshold power densities apporoximately 30-40% lower than the comparable UG structure.

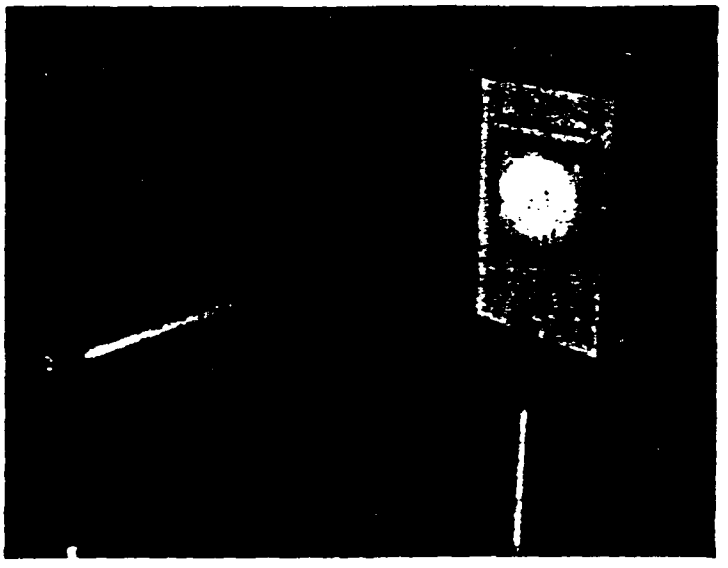

Fig.III.5 Photo of the infrared laser beam emitted from sample. The laser is the small bright spot at the left. The beam passes through a filter (to completely remove the pump beam) and travels to the card placed 30 cm to the right.

To ultimately make our devices practical, we need to have a way of electrically contacting them. We have developed a fabrication process which provides carrier injection to the active region by doping the top mirror layers p-type and the bottom mirror layers, as well as the substrate, n-type. Contact metallization to the top p-type mirror layers poses a problem in a GaAs surface-emitting laser, because light must be collected from the surface of the wafer (since the GaAs substrate wafer is highly absorbing). Therefore, we cannot cover the area where light is emitted from the surface with metal. However, by utilizing strained-layer InGaAs quantum wells, the lasing wavelength can be increased to 0.95-1.0 μm, allowing the light to be collected through the substrate (since the substrate is transparent at these wavelengths). This allows us to completely cover the top surface with metal, making the fabrication process much simpler. Thus, developing the technology to grow high quality, conventional in-plane single QW InGaAs lasers (see section I.e) was partially motivated by the practical fabrication advantages that InGaAs quantum wells offer over standard GaAs quantum wells in surface-emitting lasers.

Fig.III.6a illustrates a cross-section of the finished laser structure which incorporates a single InGaAs quantum well. As can be seen, the lateral carrier and optical confinement are formed by etching a vertical mesa of 5-10 μm in diameter and 3-4 μm in depth. A polyimide layer insulates the top metal layer from the n-type bottom mirror in the field, while at the same time providing a sloped mesa sidewall for better step-coverage of the p-type top metallization layer at the edges of the mesa. Electrical I-V curves are shown in Fig.III.6b. We believe that the consistently high turn-on characteristics (>40 V) of these devices are due to the large heterobarriers within twenty-plus alternating GaAs/AlAs p-P junctions of the top mirror layer. The high turn-on has thus far prevented us from providing high enough current densities to see lasing behavior in these devices. We are presently working on ways to avoid this problem.

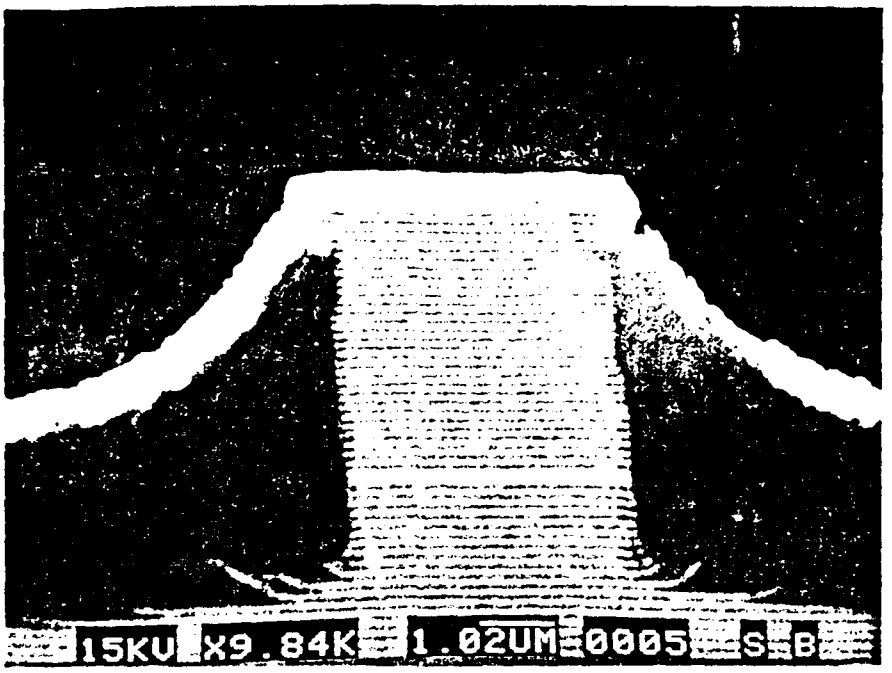

(a)

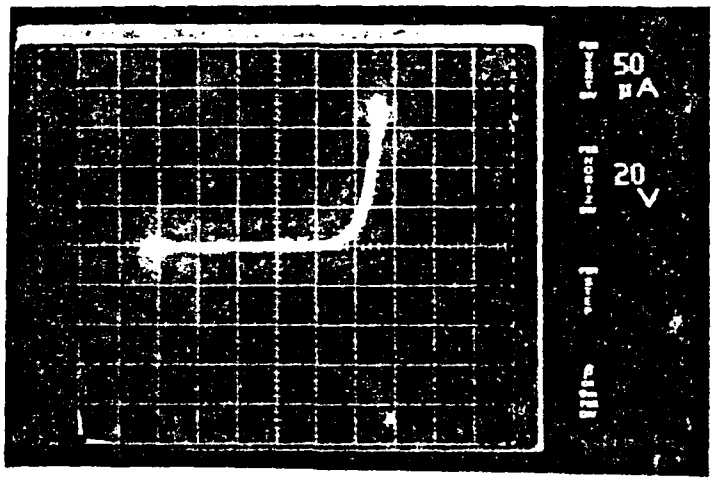

(b)

Fig.III.6 Electrical characteristics of InGaAs quantum well SEL. (a) Cross-sectional view of finished laser. RIE etched mesa with a polyimide insulating layer and metal contact pad can be clearly seen. (b) I-V curve for the structure.

References for section III:

[III.1] "Electrically tunable Fabry-Perot mirror using multiple quantum well index modulation," R.J. Simes, R.H. Yan, R.S. Geels, L.A. Coldren, J.H. English, A.C. Gossard, and D.G. Lishan, Appl. Phys. Lett. 53, 637 (1988).

[III.2] R. Geels, R. H. Yan, J. W. Scott, S. W. Corzine, R. J. Simes, and L. A. Coldren, "Analysis and Design of a Novel Parallel-Driven MQW-DBR Surface-Emitting Diode Laser," *CLEO'88,* Anaheim, CA, April 25-29, 1988, paper WM1.

[III.3] S. W. Corzine, R. S. Geels, J. W. Scott, and L. A. Coldren, "Surface-Emitting Lasers with Periodic Gain," *LEOS'88,* Santa Clara, CA, November 2-4, 1988, paper OE1.2.

[III.4] S. W. Corzine, R. S. Geels, J. W. Scott, R. H. Yan, and L. A. Coldren, "Design Of Fabry-Perot Surface-Emitting Lasers with a Periodic Gain Structure," *IEEE J. Quantum Electron.,* vol. QE-25, no.6, 1989.

[III.5] S. W. Corzine, R. S. Geels, J. W. Scott, R. H. Yan, and L. A. Coldren, and P. L. Gourley, "Efficient, Narrow-Linewidth Distributed-Bragg-Reflector Surface-Emitting Laser with Periodic Gain," *IEEE Photonics Tech. Lett.,* vol. 1, pp. 52-54, 1989.

[III.6] P. L. Gourley, T. M. Brennan, B. E. Hammons, S. W. Corzine, R. S. Geels, R. H. Yan, J. W. Scott, and L. A. Coldren, "High-efficiency TEM_{00} continuous-wave (Al,Ga)As epitaxial surface-emitting lasers and effect of half-wave periodic gain," *Appl. Phys. Lett.,* vol. 54, pp.1209-1211, 1989.

[III.7]S.W.Corzine, R.S.Geels, J.W.Scott, and L.A.Coldren, "Experimental Comparison between Periodic Gain and Uniform Gain Surface-Emitting Lasers by Optical Pumping," to be presented at *IOOC'89,* Kobe, Japan, July 18-21, 1989.

IV. Novel Waveguide Devices

a. Impurity-free disordering of GaAs/AlGaAs quantum well structures

1. Motivation:

By disordering, that is by interdiffusing Al and Ga in a quantum well, one can make the band gap of the structure larger and the refractive index smaller. If this can be achieved locally on a sample, then the disordering can be used to provide lateral confinement in waveguides. Moreover, the disordered section is transparent at the lasing wavelength of the as-grown (non disordered) section. Therefore, disordering makes possible the monolithic integration of butt-coupled laser and transparent waveguide, from a single epitaxy. If the quality of the material after disordering is such that the shift of the absorption edge under electric field (the so called Quantum Confined Stark Effect) is still efficient, phase modulation is possible as well. Of course, taking advantage of the conventional linear electro-optic effect (Pockels effect) may reinforce this quadratic effect. We are reporting here how the two necessary conditions, disordering and selectivity of the disordering have been obtained, for two different techniques: Argon implantation and thermal annealing of samples covered with various caps.

2. Argon Implantation:

The test structure is shown on Fig. IV.1. A separate confinement structure is used which is made of four QW's in a 20% Al waveguide, itself embedded in 40% Al cladding layers. The energy of the Ar ions is 3MeV and the dose, 7e14 cm^{-2}. An anneal of 850°C for 30 minutes recovers damage after implantation.

Cathodoluminescence was measured, showing a very large "blue" shift of 100 meV in energy, that is about 500 Å in wavelength (Fig.IV.2). The largest peak visible on the "as-grown sample" curve is due to some spreading of the electron beam in the partially disordered region which separates the implanted from the unimplanted section.

Waveguide loss at 1.15 μm measured in unimplanted and implanted regions was 15 and 25 cm^{-1} respectively. In both cases, the measurement was made at a wavelength far from the

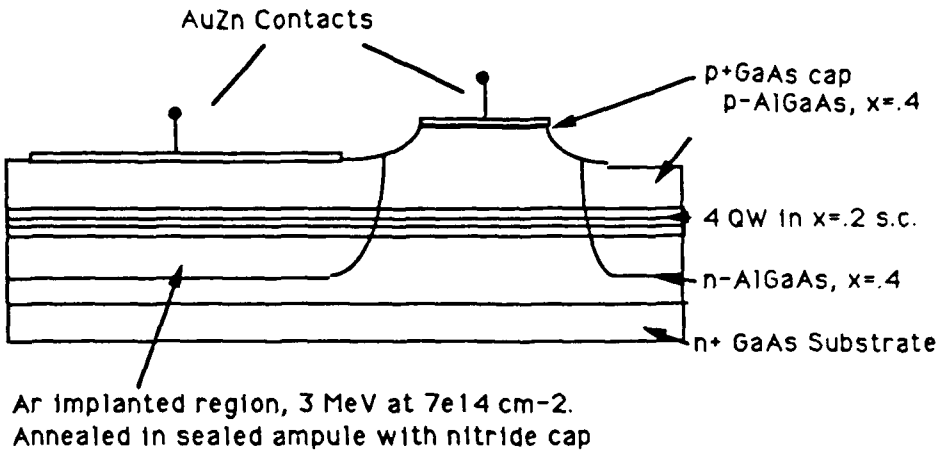

Fig. IV. 1. Test structure after implantation

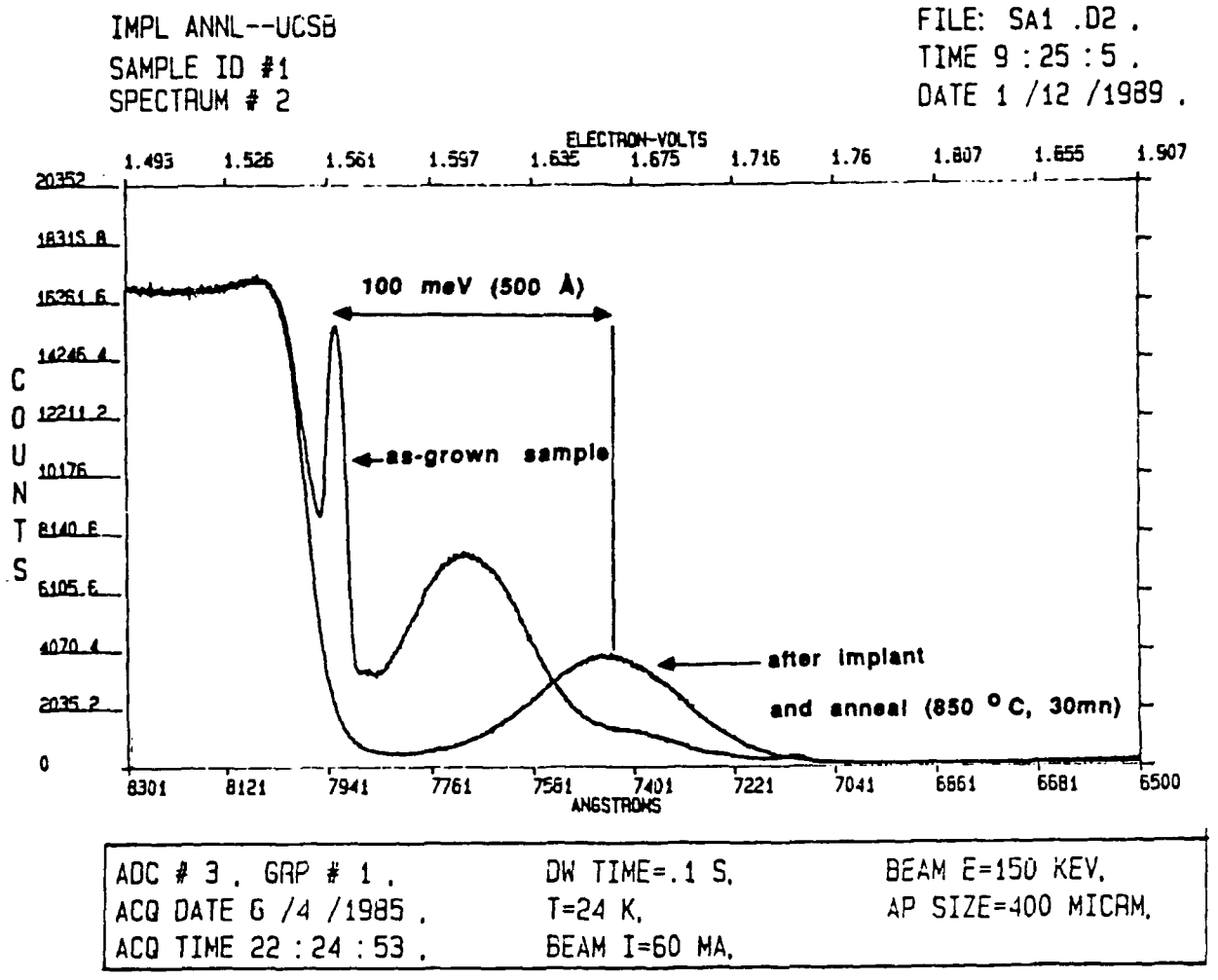

Fig. IV. 2. Cathodoluminescence after implantation

band edge, and makes it possible to compare the quality of the material before and after implantation. Although damaged, the disordered material has been successfully used as a lateral confinement layer in a planar waveguide. At 1.15 μm, loss in unimplanted waveguides was independent of stripe width, yet was single mode for stripe-widths up to 8 μm. Moreover, by decreasing the dose of implanted ions, and therefore the disordering, one should also reduce the damage, making this technique more attractive for integration of a laser and waveguide.

3. Thermal annealing:

The same 4 QW structure is used here. Before annealing, photoluminescence reveals a free exciton peak at 8500 Å, with a line width (FWHM) of 10 Å (2 meV). Photoluminescence was measured again after annealing at 800, 850 and 900°C for various times[Fig IV.3]. No significant disordering was observed at 800°C, in the range of 1 hour of annealing. At 850 and 900°C, the enhancement of the disordering is obvious under the SiO_2. Nevertheless, at 900°C, the very large blue shift always comes together with a very broad line width, which indicates the poor uniformity in thickness, after annealing. Good selectivity is measured after annealing 50min at 850°C. No shift is observed under the SiN, which seals the surface[IV.1], whereas an 80 Å blue shift is observed under the SiO_2. Under both caps, the luminescence peak slightly broadens, by 8 and 11 Å, respectively.

To make devices, contacts were electroplated on the non-annealed sample: 50 μm wide Platinum stripes on the p side and Indium on the back side. After lapping and cleaving, devices were tested as lasers under pulsed excitation. Before annealing, the threshold current density was 700 A / cm ^{2} and the measured wavelength was λ_{NA} = 8650 Å, which represents a shift of 150 Å from the exciton peak. To selectively disorder one section of the sample, a 1000 ÅSiN layer is deposited by Plasma Enhanced C.V.D(PECVD). Then, a step of photoresist (parallel to a cleaved facet), is used to partially mask the dielectric, before etching with a CF_4 plasma. After removing the photoresist, a 1000 Å SiO layer is deposited by

PECVD[Fig.IV.4]. Finally, the sample is annealed in sealed ampule, with an overpressure of As, at 850°C for 50min. Again, a 80 Åselective blue shift is observed, under the SiO_2 while no shift is measured under SiN. The integration of a laser and modulator on this sample is in progress.

Some further measurements were made on the sample annealed 1H at 850°C, taken from the same wafer. Under the SiO_2 the shift is very large (330 Å), but the broadening of the luminescence peak is also large (80 Å) and lasing could not be obtained from the sample. Nevertheless, on the SiN capped sample, a 100 Å blue shifted peak is measured (excitonic peak at 8400 Å), with a 26 Åline width. Broad area contacts were deposited, and laser fabrication and testing as well as photoconductivity measurements were carried out. Our purpose was to check the quality of the material in that range of disordering. The threshold current density was 620 A / cm^2. Although the lasers were processed from the same wafer, some inhomogeneity across the sample may explain the slight decrease. Such a result demonstrates that the annealing does not affect the laser properties. The wavelength, λ_A = 8500 Å, is shifted by 100 Åfrom the exciton,compared to 150 Åfor the non-annealed sample. The difference is not yet clearly understood, although the change in well shape is the probable cause. In our photoconductivity measurement set-up, the beam is normal to the surface of the sample and the photocurrent at room temperature is recorded versus wavelength,(Fig.IV.5a), before and after annealing. The 100 Å shift is consistent with the PL measurement. Indeed, the heavy and light hole exciton are still resolved after annealing[IV.2]. Moreover, the red shift under reverse bias (QCSE) is clearly observed on Fig.IV.5b. The lamp which is currently used has a low power and the signal to noise ratio becomes too small for a quantitatively valid recording beyond -3V, where the dark current increases rapidly. Nevertheless, until -3V, which corresponds to a perpendicular field of about 100kV, the amplitude of the Stark shift is comparable on the annealed and non annealed sample. This indicates that the PIN diode is preserved by the thermal annealing.

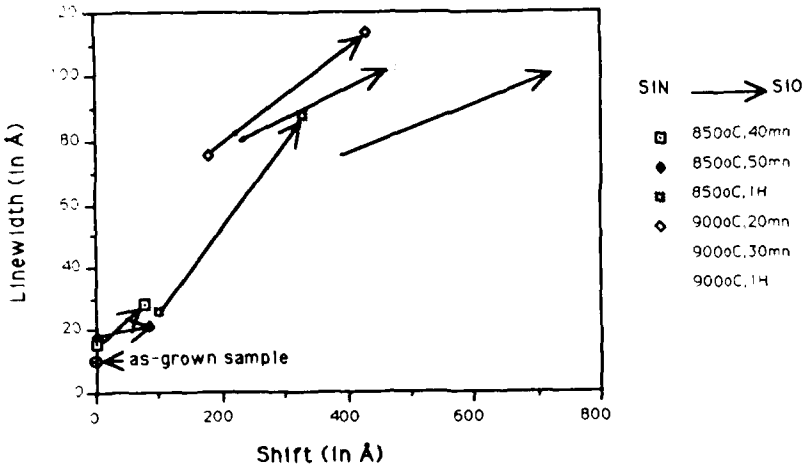

Fig. IV. 3. Summary of photoluminescence data at 1.4K for various conditions of annealing.

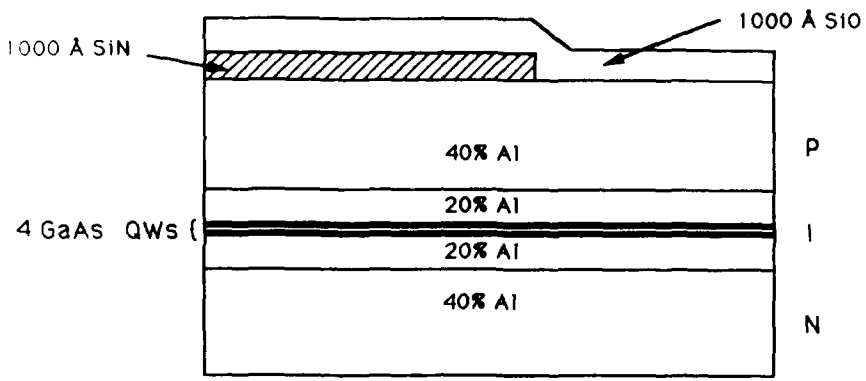

Fig. IV. 4. Schematic of the capped sample, before annealing.

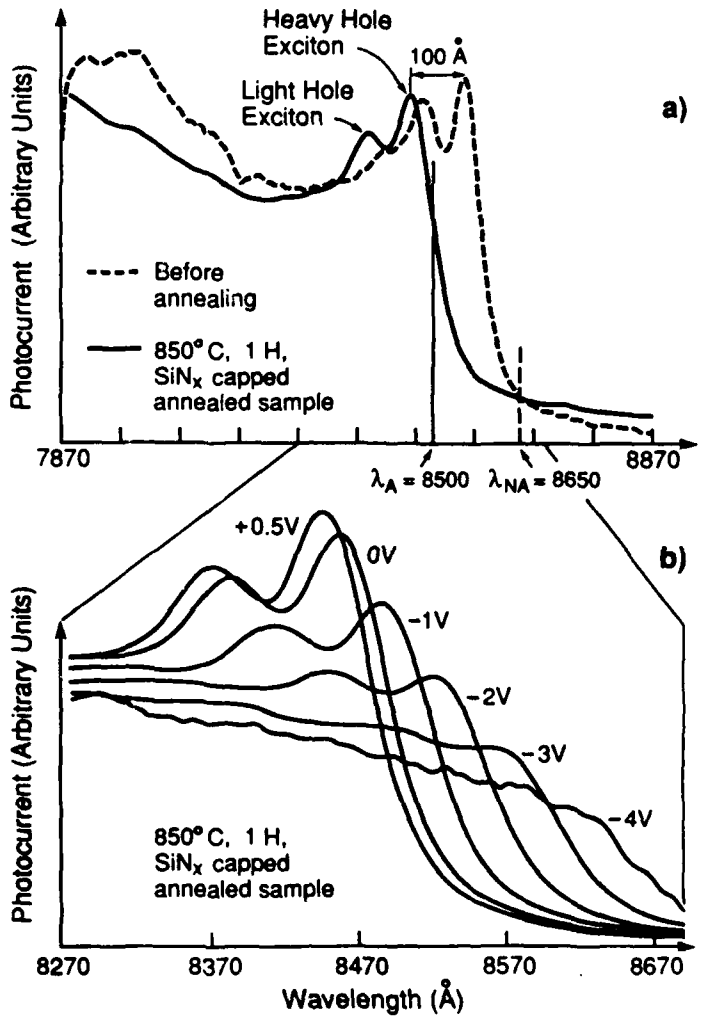

Fig. IV. 5. Photoconductivity versus wavelength for 4 x 100 Å GaAs wells with 20% Al barriers.
a- as-grown and disordered sample: no bias applies
b- disordered sample under increasing reverse bias

4. Conclusions:

Two techniques have been used to selectively disorder one section of a GaAs/AlGaAs Multiple Quantum well (MQW) structure:

- Planar monomode waveguides have been fabricated where the Argon implanted region provides the lateral confinement. Yet, in our experimental conditions, with a very large disordering, the material losses are still too large for the implanted area to be used as the core of a waveguide. Lower energy or dose might be more suitable for this application.

- A permanent blue shift of the band edge of 100 Å, localized in one section of a wafer has been achieved by thermal annealing of a MQW sample, with a surface partially capped with SiN (laser) and with SiO (modulator). On both sections, the photoluminescence peak is only slightly broadened. Moreover, laser properties as well as the Quantum Confined Stark Effect are preserved, even in the disordered section, which indicates that the as-grown P-N junction is retained. Therefore, the investigated process should be highly suitable for the monolithic integration of a laser and phase modulator.

b. Depletion Edge Translation Optical Switch

Optical switches are key components in optical transmission networks or optical signal processing[IV.3, IV.4]. For this reason, making high-speed, high-extinction-ratio, small photonic switches is attracting more and more attention. A couple of years ago, we proposed an AlGaAs/GaAs X-crossing optical switch which uses the concept of reflection from a depletion edge that can be translated across the waveguide. This structure provides a sharp and well defined impedance discontinuity as well as benefiting from carrier related effects by using doped active regions.

The schematic diagram of the switch is shown in Fig.IV.6a. To switch light between the transmission guide and the reflection guides, it is necessary to have an impedance discontinuity variation at the intersection of the two waveguides. It can be seen from the diagram that the p-n junction is formed at the cross section of the two waveguides. When a reverse bias is applied,

the depletion edge of the p-n junction will sweep across the guide layer; that is, the depletion width in the guide layer can be controlled by the applied reverse bias. So the effective refractive index in the guide layer to the right will change because of the modulation of the depletion region. Due to this impedance discontinuity, a reflection occurs and is controlled by changing the reverse bias. Therefore, the incident light power *P1* can be switched between *P2* and *P3* by the reflection, and the ratio of the transmitted light *P2* to the reflected light *P3* depends on the applied reverse bias.

The switch was fabricated on an n+ GaAs wafer by growing a double heterostructure using MBE (Molecule Beam Epitaxy). To create the impedance discontinuity, silicon ions were implanted at 70 keV and at 370 keV, each at a fluence of $5x10^{14}$ cm^{-2}, and rapid annealed at $920^{o}C$ for 15 second into the areas indicated on Fig.IV.6b.After implantation and annealing, 5 μm wide ridge waveguides whose X-crossing angle 2Øwas about 6.8^{o} were formed by using a Br: HBr wet etch. A window was opened through the SiO2 film for the p region electrode.

At 1.06 μm, the switch exhibits a contrast ratio of more than 2:1 for the TE mode at both transmission and reflection guides when the applied reverse bias is switched from 0 to -8 volts. Fig. IV.7a shows the changed output light intensity *P2* and *P3* as functions of the applied voltage[IV.5]. To better approximate a plane wave situation, similar Y-branch multimode switches which have multimode 20 μm wide guides have been fabricated and measured. Also, the output light from the straight guide and from the Y-branch was observed as a function of the applied reverse bias. Fig. IV.7b shows the change of the output light intensity vs. applied voltages for the multimodes[IV.6]. It can be seen from Fig. IV.7a and Fig. IV.7b that the on-off ratio for the multimode device is higher than that of the single mode device. It is believed that the differences between the k-spectrum, that is, the plane wave composition, for multimode and single mode, and modal interference for the multimode case are involved.

Some initial calculations have been done based on Fourier expansion techniques [IV.7] to verify the experimental results. Agreement between calculated and experimental results is not

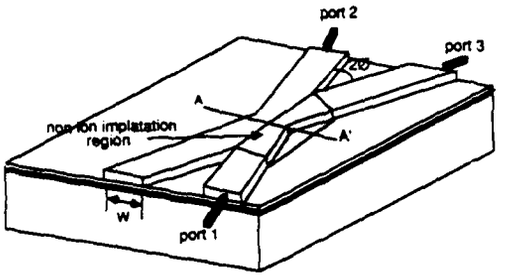

(a)

Fig. IV. 6(a) Schematic diagram of the switch. A planar p-n junction remains in the shaded region that was masked from the Si implantation. This allows for a controlled change in the effective index there and therefore the reflection at the edge of the region.

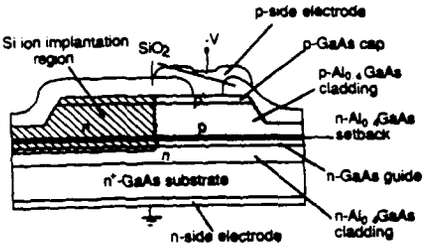

(b)

Fig. IV. 6(b) Cross-section through points A-A' of fig.1(a). The guide layer is 0.2μm thick, the set back layer is 0.1μm thick, the n-Al0.4GaAs cladding layer is 1μm, and the dope concentrations for those layers are 2x1017cm-3. P-Al0.4GaAs layer is 0.45μm, 5x1017cm-3. Guided light is reflected at the intersection of the left and right regions, and is controlled by the change in the effective index in the right side.

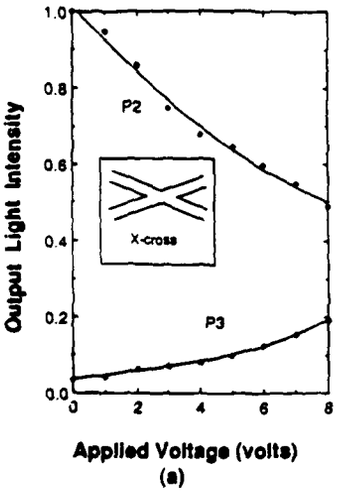

(a)

Fig. IV. 7(a) Output light intensity change from the transmission guide (P2) and from the reflection guide (P3) vs. the applied reverse bias for the X-crossing single mode switch.

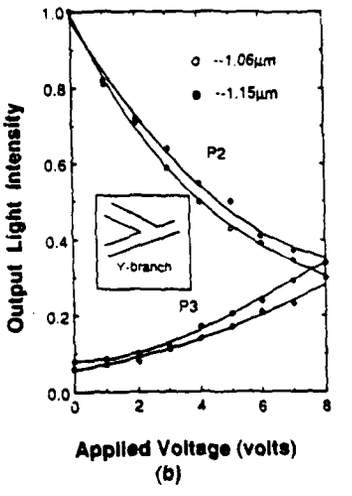

(b)

Fig.IV. 7(b) Output light intensity change from the transmission guide (P2) and from the reflection guide (P3) vs. the applied reverse bias for the Y-branch multimode switch.

very good which is probably because the calculation did not take into account a number of secondary boundaries between the input and output planes. However, from the calculation, it was found that the performance of the switch can be improved by further optimizing the thickness of the set back layer to have a small crosstalk and high reflection, by adjusting the doping concentration and the thickness of the guide layer, or by using modulation-doped quantum-well effects to cause large refractive index changes.

c. Waveguide Phase Modulators

Progress in double heterostructure (DH) waveguide phase modulators has led to studies of a similar structure using quantum wells, and finally to a comparison between the two devices in terms of phase shift efficiency and the chirp parameter.

Initial work with double heterostructure (DH) waveguide phase modulators used for the first time a Depletion Edge Translation (DET) technique by including both field and carrier effects to achieve what are still the largest phase shift efficiencies reported for GaAs/AlGaAs DH phase modulators (~100 °/Vmm at 1.06 μm) [IV.8-IV.12]. A theoretical analysis of this DH phase modulator compared two designs, one with a pn junction at the edge of a waveguide and one with the junction in the center of the waveguide, and including the effect of doping levels in the active region [IV.13-IV.15]. For the first time, the phase shift efficiency was characterized as a function of voltage and wavelength with respect to all of the different effects causing the change in index (see Fig. IV.8-IV.9). Finally, we calculated the relative change in absorption due to these same effects and noted that one could design a modulator with π phase shift (at an operating voltage of 0 to -5 V) and less than 3 dB of absorption modulation at wavelengths longer than 0.99 μm in GaAs.

We also showed that waveguide phase modulators could be fabricated using impurity induced disordering (IID) technology [IV.16-IV.17]. This allows for integration with lasers using a similar technology and planar structures. Two methods were used: one method used diffusion from a planar surface into a DH modulator structure, and the other used diffusion into

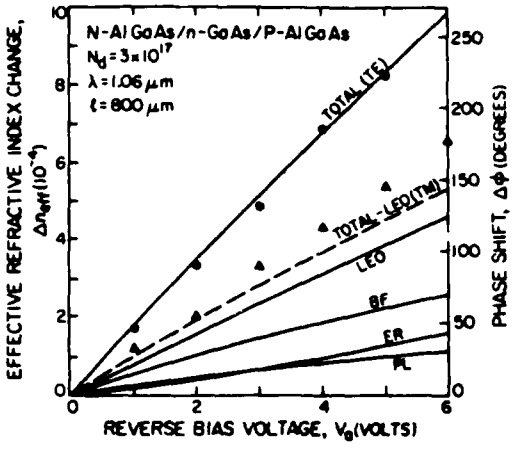

Fig. IV. 8. Voltage dependence of the effective refractive index variation and the corresponding phase shift for the device with the junction at the edge. Lines correspond to the theoretical calculations assuming a wavelength of 1.06μm and a device length of 800μm to obtain the phase shift. Four contributions to the total phase shift are shown: LEO (linear electrooptic effect), ER (electrorefractive effect), PL (plasma effect), and BF (band-filling effect). Experimental points from [1] are shown as dots for the TE mode and triangles for the TM mode. No fitting parameters were used in the theoretical calculations.

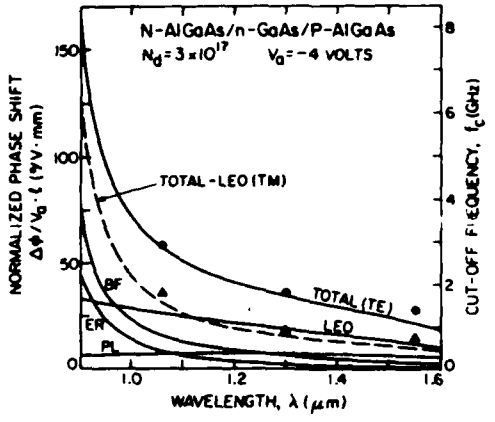

Fig. IV. 9. Wavelenth dependence for the normalized phase shift of a device with the junction at the edge, assuming a doping in the waveguide of 3 x 10^{17} cm^{-3} and a reverse bias of 4 V. Experimental points for the TE mode (solid points) and the TM mode (triangles) are shown from [5]. For wavelengths close to the bandgap, ER and BF effects becomes more important than the LEO effect. For $\lambda = 0.9$ μm, efficiencies of up to ~170°/V • mm are predicted. Right-hand axis gives the small signal cutoff frequency for a 3-μm waveguide width, a load resistance of 50 Ω, and length of L_π at $V_\pi = 4$ V.

the sides of a ridge formed in a single quantum well (QW) structure with an undoped active region (see Fig. IV.10). This work showed that the modulators were as efficient and no more loss than for wet-etched ridge technology (see Fig. IV.11).

It was pointed out that by increasing the number of quantum wells in a modulator the efficiency increases, but the ratio of phase modulation to absorption modulation decreases [IV.18]. This is measured by the chirp parameter (α_C) and it was shown that for devices integrated within a laser cavity the optimum number of wells may be 2-4 to have an efficient modulator but still allow lasing. For stand alone devices, one would want as many wells as possible, to improve the efficiency (see Fig. IV.12), since an adequate chirp parameter (α_C>10) is obtained at about the same wavelength anyway (wavelengths greater than ~0.89 μm).

Finally, we compared the DH DET design to the QW design with respect to efficiency and the chirp parameter. Initial results indicated that the chirp parameter increases to an adequate level for phase-dominant modulation (α_C>10) nearer to the absorption edge and more abruptly for the QW design than for the DH design (see Fig. IV.13) [IV.19]. At this boundary point, the phase shift efficiencies are roughly equal, but the possibility of working nearer to the band edge is encouraging for integration with lasers.

d. Impurity Induced Disordered Laser by Self-aligned Si-Zn diffusion

Quantum well lasers by impurity-induced disordering (IID) are very attractive for application to OEIC's due to its very low threshold current and its relatively simple fabrication procedures. Good IID lasers with threshold currents as low as 3 mA made by Si diffusion disordering have been reported[IV.20]. However, the laser structure itself still requires complicated fabrication procedures involving selective etching of the top contact layer and critical alignment to obtain lateral current confinement. In order to simplify the laser fabrication, a possible approach is to design a structure which can employ the technology of self-aligned Si-Zn diffusion developed recently[IV.21].

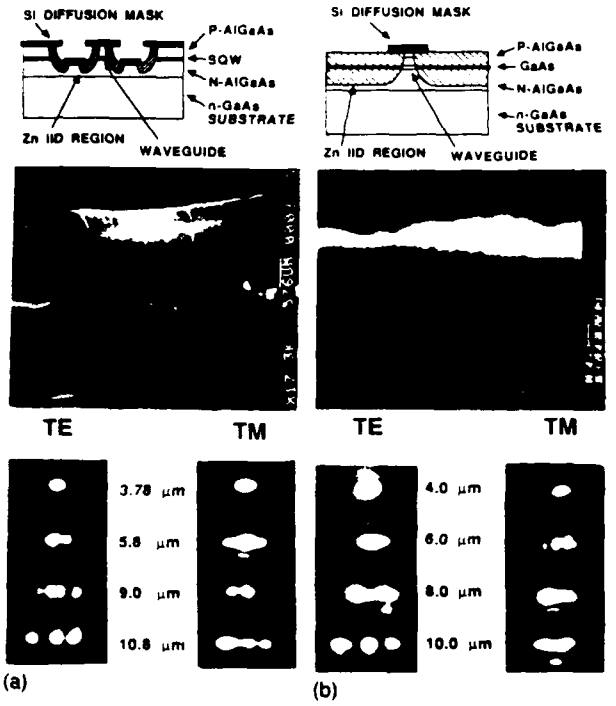

Fig. IV. 10. Device schematics (top, SEM cros sections (center), and near-field mode patterns (bottom) for (a) MBE-grown SQW waveguide, and (b) LPE-grown DH waveguide. The GaAs regions have been stained with superoxol (H_2O_2 based etch). Guide widths as measured in the SEM are indicated for each mode profile. Single-mode propagation was observed for guides less than 4-6μm width.

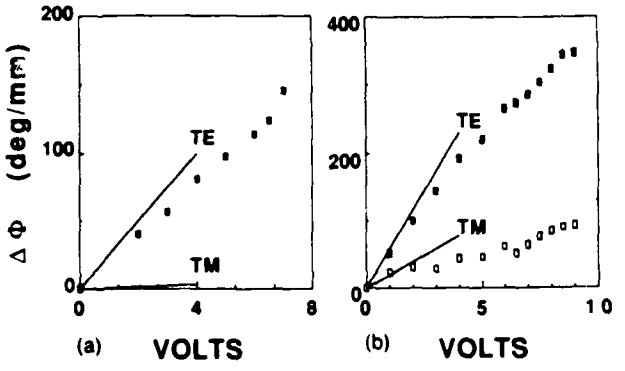

Fig. IV. 11. Normalized phase shift at 1.15μm for TE and TM polarizations vs applied voltage for (a) the MBE SQW device, and (b) the LPE DH device. Theoretical estimates are shown by solid lines. The TM measurement for (a) was too small to measure, as expected.

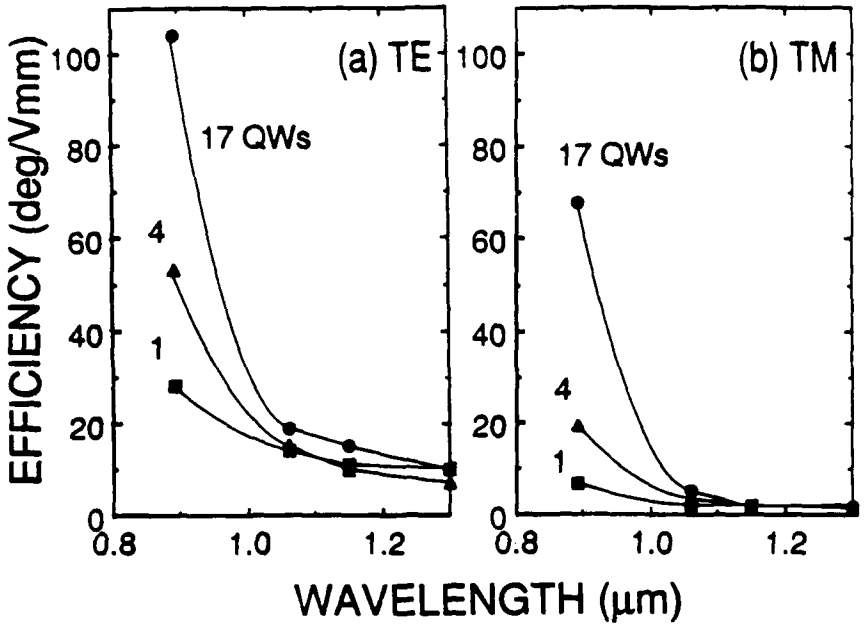

Fig. IV.12. Experimental results for phase modulation efficiency as a function of wavelength for three quantum well structures and for TE (a) and TM (b) polarizations. Data were taken between 0 and -5 V. The curves serve only to aid the eye.

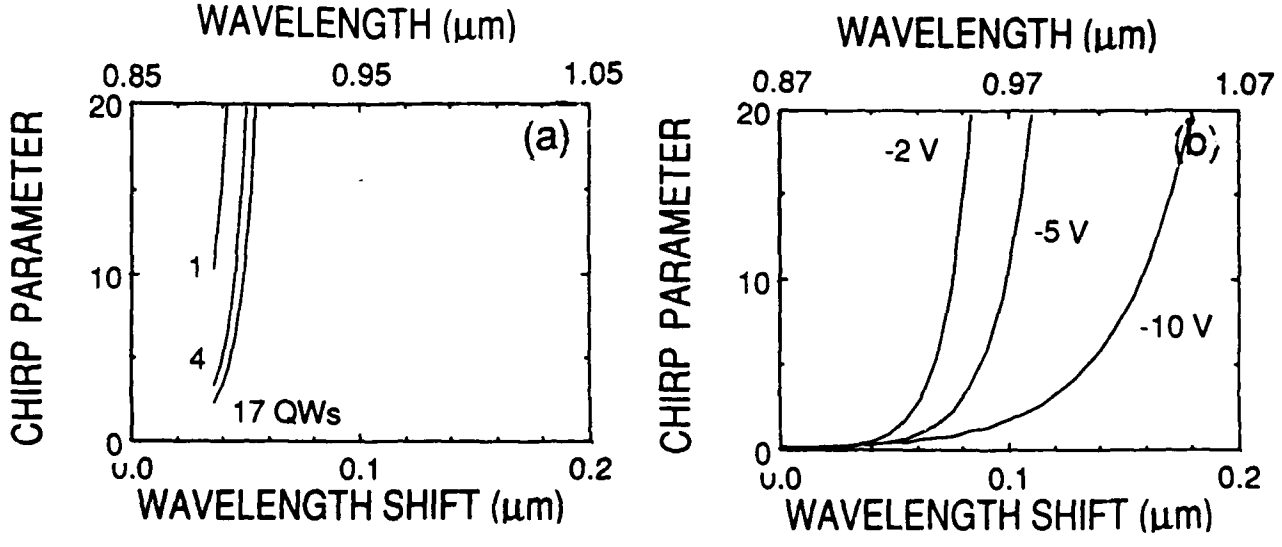

Fig. IV.13. The chirp parameter (ac) shown as a function of wavelength and the shift in wavelength from each absorption edge. The three QW cases are presented in (a) at -2 V and the DH case is presented in (b) for -2, -5, and -10 V.

We speculated that the top GaAs layer (see Fig.IV.14), which is necessary to facilitate the ohmic contact, will become a larger band gap material $(Si_2)_x(Al_yGa_{1-y}As)_{1-x}$ after Si diffusion if the thickness is less than 1000Å. Therefore, it is not necessary to worry about the leakage current through the p-n junction in the top GaAs layer; and IID novel lasers, which require simpler fabrication procedures and have better laser stripe width control due to a direct compatibility with the technology of self-aligned Si-Zn diffusion, have been developed. Good lasers with low threshold currents (20mA) and high yield (>70%) have been demonstrated by our initial attempts (see Fig.IV.15) .

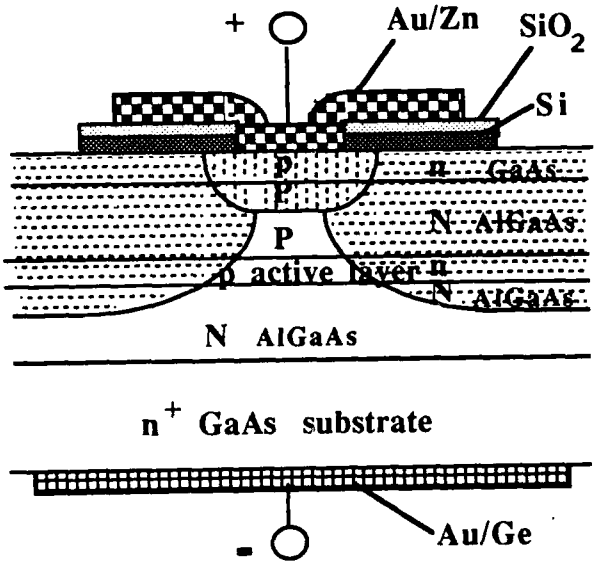

Fig. IV 14. Laser Structure

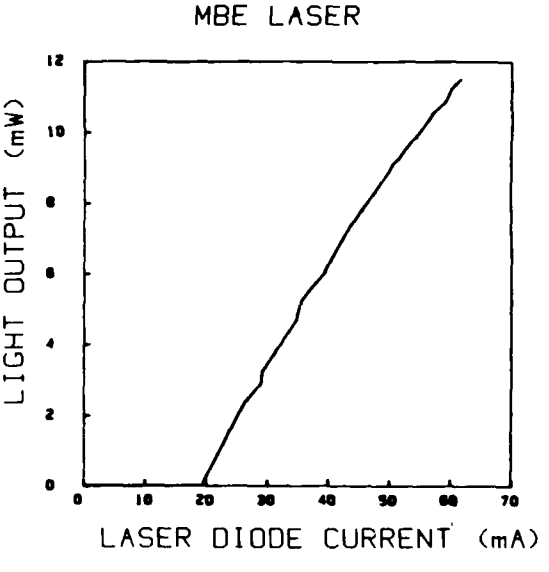

Fig. IV. 15. Laser Characteristics

References for section IV:

[IV.1] L.J. Guido, N. Holonyak, Jr., K.C. Hsieh, R.W. Kaliski, W.E. Plano, R.D. Burnam, R.L.Thornton, J.E. Epler and T.L. Paoli " Effects of dielectric encapsulation and As overpressure on Al-Ga interdiffusion in $Al_xGa_{1-x}As$- GaAs quantum-well heterostructures," *J. Appl. Phys.*, 61(4), 15 February 1987, pp. 1372-1379.

[IV.2] H. Ribot, K.W. Lee, R.J. Simes, R.H. Yan and L.A. Coldren "Disordering of GaAs/AlGaAs Multiple Quantum Well Structures by Thermal Annealing for Monolithic Integration of laser and Phase Modulator" Submitted to *Applied Physics Letters*.

[IV.3] S.D.Personic, "An engineering perspective on the application of photonic switching technology", *IEEE Global Telecommunication Conference*, pp. 871-873, 1984.

[IV.4] P.W.Smith, "On the Role of Photonic Switching in Future Communications Systems", *IEEE Circuits and Devices Magazine*, 3, pp. 9-14, 1987.

[IV.5] T.C.Huang, T.Hausken, K.Lee, N.Dagli, L.A.Coldren, D.R.Myers, "Depletion Edge Translation Waveguide-Crossing Optical Switch", *Photonics Technology Letters*. July 1989

[IV.6] T.C.Huang, K.Lee, T.Hausken, N.Dagli, L.A.Coldren, D.R.Myers, "An Optical Modulator/Switch Using The Reflection From A Translated Depletion Edge" 1989 Integrated and Guided Wave Optics Conference (IGWO).

[IV.7] J.Nayyer, Y.Suematsu, K.Shimomura, " Analysis of Reflection-Type Optical Switches with Intersecting Waveguides", Journal of Lightwave Technology, Vol.6. No. 6, June 1988, pp. 1146-1152

[IV.8] X.S. Wu, A. Alping, A. Vawter, and L.A. Coldren, "Miniature optical waveguide modulator in AlGaAs/GaAs using carrier depletion", *Electron. Lett.*, 22 (13 Mar 1986) p. 328.

[IV.9] A. Alping, X.S. Wu, T.R. Hausken, and L.A. Coldren, " Highly efficient waveguide phase modulator for integrated optoelectronics", *Appl. Phys. Lett.*, 48 (12 May 1986) p. 1243.

[IV.10] A. Alping, X.S. Wu, and L.A. Coldren, "Wavelength dependence of high-performance AlGaAs/GaAs waveguide phase modulators", *Electron. Lett.*, 23 (15 Jan 1987) p. 93.

[IV.11] A. Alping and L.A. Coldren, "Electrorefraction in GaAs and InGaAsP and its application to phase modulators", *J. Appl. Phys.*, 61 (1 Apr 1987) p. 2430.

[IV.12] J.G. Mendoza-Alvarez, R.H. Yan, and L.A. Coldren, "Contribution of the band-filling effect to the effective refractive index change in double-heterostructure GaAs/AlGaAs phase modulators", *J. Appl. Phys.*, 62 (1 Dec 1987) p. 4548.

[IV.13] L.A. Coldren, J.G. Mendoza-Alvarez, and R.H. Yan, "Design of optimized high-speed depletion-edge-translation modulators in III-V semiconductors", Appl. Phys. Lett., 51 (14 Sept 1987) p. 792 and 52 (11 Jan 1988) p. 169.

[IV.14]J.G. Mendoza-Alvarez, L.A. Coldren, A. Alping, R.H. Yan, T. Hausken, K. Lee, and K. Pedrotti, "Analysis of depletion edge translation lightwave modulators", Jour. Lightwave Tech., 6 (June 1988) p. 793.

[IV.15] T. Hausken, K. Lee, R. Simes, R Yan, J. Mendoza-Alvarez, N. Dagli, L.A. Coldren, and K. Pedrotti, "Optical waveguide phase modulators in AlGaAs/GaAs with very high figures of merit", *IEEE Device Research Conference* (June 1987) paper IIIA-3.

[IV.16]T.R. Hausken, T.C. Huang, K.W. Lee, R.J. Simes, N. Dagli, and L.A. Coldren, "Phase modulation in impurity induced disordered AlGaAs/GaAs quantum well and double heterostructure waveguides", 1988 Integrated and Guided Wave Optics Conference (IGWO), Santa Fe, NM, paper MA3.

[IV.17] T. Hausken, T.C. Huang, K.W. Lee, R.J. Simes, N. Dagli, and L.A. Coldren, "Impurity induced disordered phase modulators in AlGaAs/GaAs quantum well and double-heterostructure waveguides", Appl. Phys. Lett., 53 (29 Aug. 1988) p.728.

[IV.18] T. Hausken, R.H. Yan, R.J. Simes, and L.A. Coldren, "Relating the chirp parameter to the number of quantum wells in GaAs/AlGaAs waveguide modulators", submitted to Appl. Phys. Lett. 10 Apr. 1989.

[IV.19] T. Hausken, K.W. Lee, R.J. Simes, R.H. Yan, and L.A. Coldren, "Dependence of chirp on the number of wells in GaAs/AlGaAs waveguide modulators", 1989 Integrated and Guided Wave Optics Conference (IGWO) Houston, TX, paper WAA2.

[IV.20] D.G. Deppe, K.C. Hsieh, and N. Holonyak, Jr. J. Appl. Phys. 58, 4515 (1985).

[IV.21] W.X. Zou, S. Corzine, G.A. Vawter, J.L. Merz, L.A. Coldren, and E.L. Hu, J. Appl. Phys. 64, 1855 (1988).

C. Conference and Journal Publications

I. Primarily Funded by ARO

[1] R.S. Geels, S.W. Corzine, J.W. Scott, R.J. Simes and L.A. Coldren, "A Vertical Array Large-Optical-Cavity Laser," *LEOS'88*, Santa Clara, CA, paper OE2.4 (November 1988).

[2] S.W. Corzine, R.S.Geels, J.W. Scott and L.A. Coldren, "Surface-Emitting-Lasers with Periodic Gain," *LEOS '88*, Santa Clara, CA , paper OE1.2 (November 1988).

[3] I. Suemune, L.A. Coldren, M. Yamanishi and Y. Kan, "High-Speed Modulation Capability and Low Threshold Current Density in Strained Quantum-Well Laser Structures," *Conf. on Solid State Devices and Materials*, Tokyo, (Aug. 1988), 339-342; and Conference abstract, 148b, *IQEC '88*, Tokyo, Japan, (July 1988).

[4] I. Suemune and L.A. Coldren, "Band Mixing in the Valence-Band of a Quantum Wire Structure and Excitonic Contribution to Refractive-Index," *IQEC '88*, Tokyo, Japan, paper TuG 4 (July 1988).

[5] I. Suemune and L.A. Coldren, "Band Mixing Effects and Excitonic Optical Properties in Quantum Wire Structures - Comparison with the Quantum Wells," *IEEE Journal of Quantum Electronics*, **24** (8), 1778-1790 (August 1988).

[6] M. Tsuchiya, J.M. Gaines, R.H. Yan, R.J. Simes, P.O. Holtz, L.A. Coldren and P.M. Petroff, "Observation of Polarization Dependence of Absorption in a Quantum-Well Wire Array Grown Directly by Molecular Beam Epitaxy," *J. of Vac. Science & Technology*, **7**, (2), 315-318 (March/April 1989); *9th Molecular Beam Epitaxy Workshop*, West Layfayette, Indiana, (September 1988).

[7] M. Tsuchiya, J.M. Gaines, R.H. Yan, R.J. Simes, P.O. Holtz, L.A. Coldren and P.M. Petroff, "Optical Anisotropy in a Quantum Well Wire Array with Two Dimensional Quantum Confinement," *Phy. Rev. Letts.*, **62** (4) ,466 (Jan. 23, 1989)

[8] J.A. Skidmore, L.A. Coldren, J.L. Merz, E.L. Hu and K. Asakawa, "Radical Beam and Ion Beam Etching (RBIBE) of GaAs," *J. of Vac. Science & Technology*, **B6**, 1885-1888 (Nov./Dec. 1988).

[9] I. Suemune, L.A. Coldren, M. Yamanishi and Y. Kan, "Extremely Wide Modulation Band Width in a Low Threshold Current Strained Quantum Well Laser," *Appl. Phys. Letts.*, **53** (15), 1378-1381 (1988).

[10] P.M. Petroff, J.M. Gaines, M. Tsuchiya, R.J. Simes, L.A. Coldren, H. Kroemer, J.H. English and A.C. Gossard, "Bandgap Modulation in Two Dimensions by MBE Growth of Tilted Superlattices and Applications to Quantum Confinement Structures," *Journal of Crystal Growth*, **95** (1989); *5th International Conference on MBE*, Japan (September 1988).

[11] P.L. Gourley, T.M. Brennan, B.E. Hammons, S.W. Corzine, R.S. Geels, R.H.Yan, J.W. Scott, and L.A. Coldren, "High Efficiency Tem_{00} Continuous-Wave (Al,Ga)As Epitaxial Surface- Emitting Lasers and Reduced Threshold with Half-wave Periodic Gain," *Appl. Phys. Letts.* **54** (13) 1209-1211 (March 27, 1989).

[12] S.W. Corzine, R.S. Geels, R.H. Yan, J.W. Scott, L.A. Coldren, and P.L. Gourley, "Efficient, Narrow-Linewidth Distributed-Bragg-Reflector Surface- Emitting Laser with Periodic Gain," *Photonics Tech. Letts.* **1** (3) 52-54 (March 1989).

[13] M. Tsuchiya, P.M. Petroff, and L.A. Coldren, "Spontaneous Growth of Coherent Tilted Superlattice on Vicinal (100) GaAs Substrates," *Appl. Phys. Letts.* **54,** 1690 (April 24, 1989).

[14] T. Hausken, K.W. Lee, R.J. Simes, R.H. Yan, and L.A. Coldren, "Dependence of Chirp on the Number of Quantum Wells in GaAs/AlGaAs Waveguide Modulators," *IGWO '89*, paper WAA2, 199, Houston, TX (April 1989)

[15] S.W. Corzine R.S. Geels, J.W. Scott and L.A. Coldren, "Experimental Comparison Between Periodic Gain and Uniform Gain Surface-Emitting Lasers by Optical Pumping," *IOOC.*, Kobe, Japan (July 1989)

[16] T.C. Huang, K.W. Lee, T. Hausken, N. Dagli, L.A. Coldren,and D. Myers, "An Optical Modulator/Switch Using the Reflection from a Translated Depletion Edge," *IGWO '89*, paper MEE4, 98, Houston.TX (Feb. 1989)

[17] M. Tsuchiya, L. Coldren and P. Petroff, "AlGaAs/GaAs Lasers with Quantum-Wire Active Regions," *IOOC.*,Kobe, Japan (July 1989)

[18] M. Tsuchiya, L. Coldren and P. Petroff, "AlGaAs/GaAs Lasers with Quantum-Wire Active Regions," *IOOC.*,Kobe, Japan (July 1989)

[19] S. Corzine, R.S. Geels, J.W. Scott, R.H. Yan, and L.A. Coldren, "Design of Fabry-Perot Surface-Emitting Lasers with a Periodic Gain Structure," *IEEE.J. of Quantum Electronics* **25** (6), (June 1989)

[20] R.J. Simes, P.O. Holtz, F. Laruelle, L.A. Coldren, J.H. English, and A.C. Gossard, "GaAs/$Al_xGa_{1-x}As$ Lasers Grown by Molecular Beam Epitaxy at Low Substrate Temperatures," *Electronic Materials Conf.*, Boston, MA (June 1989)

[21] M. Tsuchiya, P.M. Petroff, and L.A. Coldren, "Use of Tilted-Superlattices for Quantum-Well-Wire Lasers," *47th Annual Device Research Conference* Boston, MA (June 20, 1989).

[22] L.A. Coldren, "Vertical Cavity DBR Lasers and Modulators for Optical Interconnection," *SSL'89, Bejing, China.* INVITED PAPER. (July 1989)

[23] H. Ribot, K.W. Lee, R.J. Simes, R.H. Yan and L.A. Coldren, "Disordering of GaAs/AlGaAs Multiple Quantum Well Structures by Thermal Annealing for Monolithic Integration of Laser and Phase Modulator," *submitted to Applied Physics Letters.*

[24] T.C. Huang, T. Hausken, K. Lee, N. Dagli, L.A. Coldren, "Depletion Edge Translation Waveguide Crossing Optical Switch," *submitted to Photonics Tech. Letts.*

[25] T. Hausken, R.H. Yan, R.J. Simes, and L.A. Coldren, "Relating the Chirp Parameter to the Number of Quantum Wells in GaAs/AlGaAs Waveguide Modulators," *submitted to Applied Physics Letts.*

[26] R.H. Yan, S.W. Corzine, L.A. Coldren, and I. Suemune, "Corrections to the Expression for Gain in GaAs," *submitted to IEEE Journal of Quantum Electronics*

II. Associated Publications (Partially funded by ARO)

[1] J. Maserjian, P.O. Andersson, B.R. Hancock, J.M. Iannelli, S.T. Eng, F.J. Grunthaner, K-K. Law, P.O. Holtz, R.J. Simes, L.A. Coldren, A.C. Gossard, and J.L. Merz, "Optically Addressed Spatial Light Modulators by MBE Grown nipi/MQW Structures," *Topical Meeting on Spatial Light Mod. and their Applications*, Lake Tahoe (June 1988).

[2] J.G. Mendoza-Alvarez, L.A. Coldren, A. Alping, R.H. Yan, T. Hausken, K. Lee and K. Pedrotti, "Analysis of Depletion Edge Translation Lightwave Modulators," *IEEE Journal of Lightwave Technology*, **6** (6), 793-808 (June 1988).

[3] T.R. Hausken, T.C. Huang, K.W. Lee, R.J. Simes, N. Dagli and L.A. Coldren, "Phase Modulation in Impurity-Induced-Disordered AlGaAs/GaAs Quantum-Well and Double-Heterostructure Waveguides," *Integrated & Guided Wave Optics Topical Meeting*, Santa Fe, NM, paper MA3 (March 1988).

[4] R. Geels, R.H. Yan, J.W. Scott, S.W. Corzine, R.J. Simes and L.A. Coldren, "Analysis and Design of a Novel Parallel-Driven MQW-DBR Surface-Emitting Diode Laser," *Conference on Lasers and Electro-Optics*, Anaheim, CA, paper WM1 (April 1988).

[5] R.J. Simes, R.H. Yan, R.S. Geels, L.A. Coldren, J.H. English and A.C. Gossard, "Surface-Normal Fabry-Perot Multi-Quantum Well Index Modulator," *Conference on Lasers and Electro-Optics*, Anaheim, CA, paper TuE2 (April 88).

[6] R.H. Yan, R.S. Simes, R.S. Geels, L.A. Coldren, J.H. English and A.C. Gossard, "Multi-Quantum Well Electro-Optic Modulator Using a Combination of Excitonic Index and Absorption Changes," *Device Research Conference*, Boulder, CO, paper IVB-2 (June 1988)

[7] J.A. Skidmore, L.A. Coldren, E.L. Hu and J.L. Merz, "Novel Radical Beam and Ion Beam Etching (RBIBE) of GaAs," *The 32nd Symposium on Electron, Ion and Photon Beams*, Ft. Lauderdale, FL, paper E2 (June 1988).

[8] J.A. Skidmore, L.A. Coldren, J.L. Merz and E.L. Hu, "Anisotropic Chemically Enhanced Etching of GaAs Using Independently Controllable Cl Radical and Ar Ion Beams" *Electronic Materials Conference*, Boulder, CO, paper H7 (June 1988).

[9] R.J. Simes, R.H. Yan, R.S. Geels, L.A. Coldren, J.H. English and A.C. Gossard, "Fabry-Perot Multi-Quantum Well Index Modulator," *Appl. Optics*, **27** (11), 2103-2104 (June 1988).

[10] J.A. Skidmore, L.A. Coldren, J.L. Merz, E.L. Hu and K. Asakawa, "Use of Independently Controlled Cl Radical and Ar Ion Beams for Anisotropic Chemically Enhanced Etching of GaAs," *Appl. Phys. Letts.*, **53**, 2308 (Dec. 5, 1988)

[11] T. Hausken, T.C. Huang, K.W. Lee, R.J. Simes, N. Dagli and L.A. Coldren, "Impurity-Induced-Disordered Phase Modulators in AlGaAs/GaAs Quantum-well and Double-Heterostructure Waveguides," *Appl. Phys. Letts.*, **53** (9), 728-730 (August 1988).

[12] R.J. Simes, R.H. Yan, R.S. Geels, L.A. Coldren, J.H. English and A.C. Gossard, D.G. Lishan, "Electrically Tunable Fabry-Perot Mirror Using Multi-Quantum Well Index Modulation," *Appl. Phys. Letts.*, **53** (8), 637-639 (August 1988).

[13] R.J. Simes, R.H. Yan, S.W. Corzine, J.H. English, L.A. Coldren and A.C. Gossard, "MBE-Growth Fabry Perot Multiple Quantum Well Reflection Modulator," *J. of Vac. Science & Technology*, **7** (2), 412-414 (March/April 1989); *9th Molecular Beam Epitaxy Workshop*, West Lafayette, Indiana (September 1988).

[14] L.A. Coldren, "In-Plane and Surface-Normal Waveguide Modulators: Maximizing Efficiency & Simplifying the Technology," *LEOS '88*, Santa Clara, CA, paper OE6.1 (November 1988). INVITED PAPER.

[15] Y. Okada, R.H. Yan, L.A. Coldren, J.L. Merz and K. Tada, "The Effect of Bandtailing on the Performance of GaAs/AlGaAs Optical Modulators and Switches Operated by Free Carrier Injection," *LEOS '88*, Santa Clara, CA paper OE3.3 (November 1988).

[16] Y.Okada, R.H. Yan, L.A. Coldren and J.L. Merz, "The Effect of Band-Tails on The Design of GaAs/AlGaAs Bipolar Transistor Carrier-Injected Optical Modulator/Switch," *IEEE J. of Quant. Electron.***25**, (4) , 713-719 (April 1989)

[17] T. Takamori, L.A. Coldren and J.L. Merz, "Angled etching of GaAs/AlGaAs by conventional Cl_2 reactive ion etching," *Appl. Phys. Letts.*, **53** (Dec. 19, 1988).

[18] R.H. Yan, R.J. Simes, H. Ribot, L.A. Coldren, and A.C. Gossard, "Room Temperature Two-Dimension Exciton Exchange and Blue Shift of Absorption Edge in GaAs/AlGaAs Superlattices under an Electric Field," *Appl. Phys. Letts.* (April 17, 1989)

[19] R.H. Yan, R.J. Simes, H. Ribot, L.A. Coldren, and A.C. Gossard, "Blue-Shifted Absorption Using Field-Induced Stark Localization in Superlattices," *Topical Meeting QW for Optics & Optoelectronics,* Salt Lake City (March, 1989).

[20] T. Takamori, L.A. Coldren and J.L. Merz, "A Folded-Cavity TJS Surface Emitting Laser," *IGWO '89,* paper MCC6,59, Houston TX, (Feb. 1989).

[21] R.H. Yan, R.J. Simes, and L.A. Coldren, "Analysis and Design of Surface-Normal Fabry-Perot Electro-Optic Modulators," *submitted to IEEE J. of Quantum Electronics.*

[22] R.H. Yan, R.J. Simes, H. Ribot, L.A. Coldren and A.C. Gossard, "Van Hove Type M_1 Exciton and Stark Localization Exciton in GaAs-AlGaAs Superlattices under an Electric Field," *CLEO '89,* Baltimore, MD (April 1989)

[23] R.J. Simes, R.H. Yan, D.G. Lishan, and L.A. Coldren, "High-Contrast Low-Voltage Fabry Perot Reflection Modulator," *submitted to 15th European Conference on Optical Communication.*

[24] R.H. Yan, F. Laruelle, and L.A. Coldren, "A Tight Binding Analysis on Exciton Binding Energy in Field- Induced Stark-Localized Superlattices," *submitted to Applied Physics Letters.*

[25] T. Takamori, L.A. Coldren and J.L. Merz, "A Folded-Cavity Transverse Junction Stripe Surface Emitting Laser," *submittedto Applied Physics Letters.*

[26] R.J. Simes, R.H. Yan, J.H. English, L.A. Coldren, and A.C. Gossard, "Molecular-beam epitaxy grown Fabry-Perot multiple quantum well reflection modulator," *J. of Vac. Science andTechnology B*, **7** (2), 412-414 (March/April 1989).

F. Personnel

1. Professor Larry A. Coldren, Ph.D.: Principal Investigator.
2. H. Kroemer: Associate Investigator
3. J.L. Merz: Associate Investigator
4 J.H. English: Development Engineer
5. D. Cohen: Development Engineer
6 R.S. Geels: Student
7. Mr. R.J. Simes: Student
8. S. Corzine: Student
9. T.C. Huang: Student
10. T. Hausken: Student
11. W. Zou: Student
12. J.M. Gaines: Visiting Research Engineer
13. M. Tsuchiya: Visiting Research Engineer